A Novel Biostable 3D Porous Collagen Scaffold for Implantable Biosensor

by

Young Min Ju

A dissertation submitted in partial fulfillment
of the requirements for the degree of
Doctor of Philosophy
Department of Chemical & Biomedical Engineering
College of Engineering
University of South Florida

Major Professor: Francis Moussy, Ph.D.
Yvonne Moussy, Ph.D.
Mark Jaroszeski, Ph.D.
Michael VanAuker, Ph.D.
Julie P. Harmon, Ph.D.

Date of Approval:
December 7, 2007

Keywords: implantable glucose sensor, porous scaffold, NDGA crosslinking,
microspheres, dexamethasone

UMI Number: 3326113

INFORMATION TO USERS

The quality of this reproduction is dependent upon the quality of the copy submitted. Broken or indistinct print, colored or poor quality illustrations and photographs, print bleed-through, substandard margins, and improper alignment can adversely affect reproduction.

In the unlikely event that the author did not send a complete manuscript and there are missing pages, these will be noted. Also, if unauthorized copyright material had to be removed, a note will indicate the deletion.

UMI®

DEDICATION

To my parents, who have always supported and encouraged me…

To my wife, Hee Jung, for always being there with devotion, patience and love…

To my son, Justin, a marvelous blessing…

ACKNOWLEDGEMENTS

Firstly, I would like to express my sincere gratitude to my dissertation advisor, Dr. Francis Moussy for his guidance, support, and encouragement in completing Ph.D. research project. Thank you for giving me the freedom to pursue this project and for developing my research career as a 'scientist'. I will be forever grateful to you for your generosity, kindness, and wisdom over the years. I extend my appreciation to the members of my Ph.D. dissertation committee, Dr. Yvonne Moussy, Dr. Mark Jaroszeski, Dr. Michael VanAuker, Dr. Julie P. Harmon, who encouraged and leaded me to the right directions during my Ph.D. study. I would also like to thank Dr. Michael Weng, who served as an external committee chairperson for my dissertation defense.

I would also like to thank the following for their assistance; Dr. Thomas J. Koob and Mr. Douglas Pringle for handling down their new technical knowledge; Ms. Margi Baldwin for her assistance with animal surgery; Ms. Sandy Livingston for her help with histology; Mr. Jay Bieber for his assistance with SEM analysis; Ms. Carla Webb, Ms. Cay Palez, Mr. Jamie Fargen, and Mr. Ed Van Etten for help with administrative and IT support.

I thank all of my fellow in Biosensor & Biomaterials Lab.; Leigh West, Bobby Yu Bazhang, Nathan Long, Paul Dungel, Eric Guegan, Nuvala Fomban, Jose Rey, and James Merker, and in Dr. Harmon's Lab.; Chunyan Wang, Moo Sung Kim, Kadine Mohomed. I would also like to thank Ms. Brett Montegny for her tutor to improve my presentation skills. I would also like to thank Won-Seok, Chungsik, Man Soo, Seung Ryong, Byung Ryong, my Korean friends in the USF. I am also grateful to Dr. Hyung Bae Jung and Dr. In Ho Ra, visiting professor from Korea, whose generosity, advice and encouragement.

Last but certainly not least, I especially thank my parents and parents-in-law who have always supported and encouraged me with unconditional charity and their prayer. I am grateful to my sister as well for her support. I am forever grateful to my wife Hee Jung. She is always by my side with devotion, patience, love, and constant cheers. Without her, I would not have completed this dissertation. Half percent of this Ph.D. dissertation belongs to her. I am also grateful to my sweet little son, Justin (A-rang), who is a blessing and a treasure of my heart.

NOTE TO READER

The original of this document contains color that is necessary for understanding

the data. The original dissertation is on file with the USF library in Tampa, Florida.

TABLE OF CONTENTS

LIST OF TABLES

iv

LIST OF FIGURES

LIST OF ABBREVIATIONS

ADA	American Diabetes Association
SMBG	Self-monitoring of blood glucose
CGMS	Continuous glucose monitoring system
Ag/AgCl	Silver/silver chloride
GOD	Glucose oxidase
ECM	Extracellular matrix
FBC	Foreign body capsule
SQ	Subcutaneous
IV	Intravascular
IP	Intraperitoneal
PEG	Poly(ethylene glycol)
PHEMA	Poly(hydroxyethylmethacrylate)
PU	Polyurethane
TRM	Tissue response modifiers
PLGA	Poly(lactic-co-glycolic acid)
Dex	Dexamethasone
PVA	Poly(vinyl alcohol)
VEGF	Vascular endothelial growth factor
PDGF	Platelet-derived growth factor
GA	Glutaraldehyde
HMDI	Hexamethylene diisocyanate
EDC	1-ethyl-3-(3-dimethylaminopropyl) carbodiimide
NHS	N-hydroxysuccinimide
NDGA	Nordihydroguaiaretic acid
PLLA	Poly(L-lactic acid)

UV	Ultra-violet
BSA	Bovine Serum Albumin
Dc	Degree of crosslinking
S	Sensitivity of glucose sensor
ePTFE	expended Poly(tetrafluorethylene)
LCST	Lower critical solution temperature
HPLC	High performance liquid chromatography

A Novel Biostable 3D Porous Collagen Scaffold for Implantable Biosensor

Young Min Ju

ABSTRACT

Diabetes is a chronic metabolic disorder whereby the body loses its ability to maintain normal glucose levels. Despite of development of implantable glucose sensors in long periods, none of the biosensors are capable of continuously monitoring glucose levels during long-term implantation reliably. Progressive loss of sensor function occurs due in part to biofouling and to the consequences of a foreign body response such as inflammation, fibrosis, and loss of vasculature.

In order to improve the function and lifetime of implantable glucose sensors, a new 3D porous and bio-stable collagen scaffold has been developed to improve the biocompatibility of implantable glucose sensors. The novel collagen scaffold was crosslinked using nordihydroguaiaretic acid (NDGA) to enhance biostability. NDGA-treated collagen scaffolds were stable without any physical deformation in the subcutaneous tissue of rats for 4 weeks. The scaffold application does not impair the function of our sensor. The effect of the scaffolds on sensor function and biocompatibility was examined during long-term *in vitro* and *in vivo* experiments and compared with control bare sensors. The sensitivity of the short sensors was greater than the sensitivity of long sensors presumably

x

due to less micro-motions in the sub-cutis of the rats. The NDGA-crosslinked scaffolds induced much less inflammation and retained their physical structure in contrast to the glutaraldehyde (GA)-crosslinked scaffolds.

We also have developed a new dexamethasone (Dex, anti-inflammatory drug)-loaded poly(lactic-co-glycolic acid) (PLGA) microspheres/porous collagen scaffold composite for implantable glucose sensors. The composite system showed a much slower and sustained drug release than the standard microspheres. The composite system was also shown to not significantly affect the function of the sensors. The sensitivity of the sensors with the composite system *in vivo* remained higher than for sensors without the composites (no scaffold, scaffold without microspheres). Histology showed that the inflammatory response to the Dex-loaded composite was much lower than for the control scaffold. The Dex-loaded composite system might be useful to reduce inflammation to glucose sensors and therefore extend their function and lifetime.

CHAPTER 1

INTRODUCTION

1.1. Diabetes

Diabetes is a chronic metabolic disorder in which the body loses its ability to maintain normal glucose levels. Diabetes is the 6th leading cause of death by disease and is rapidly increasing in the United States and around the world. The American Diabetes Association (ADA) estimates that at least 20.8 million or 7% of Americans have suffered from diabetes, caused by a lack or shortage of insulin, the hormone that allows glucose to enter the body's cells and be stored or used for physiological activation energy [1,2].

There are two major types of diabetes (Type I and II). Type I, or insulin-dependent diabetes, is an autoimmune disease. It is marked by blood sugar levels rising out of control because the body's immune system destroys the insulin-producing beta cells in the pancreas. The pancreas then produces little or no insulin. Approximately, 5-10% of diabetes cases in the US is Type I. Type II diabetes is the most common form of diabetes. It is characterized clinically by hyperglycemia and insulin resistance, which results when the insulin produced, does not adequately control the uptake of glucose by the cells. Type II diabetes

1

is usually the type of diabetes diagnosed in patients that are over 30 years old or obese. Ninety percent of diabetes cases is Type II [2-4].

Diabetes has acute and chronic effects on the body, and may lead to death. Persistent abnormal high levels of blood glucose can slowly damage both the small and large blood vessels in the body, resulting in numerous complications [2,3], such as:

- Heart disease and stroke

- High blood pressure

- Blindness

- Kidney disease

- Nervous system disease

- Amputations

- Dental disease

- Complications of pregnancy

- Erectile dysfunction

Thus, physicians and researchers are trying to develop better ways of monitoring and curing diabetes to avoid life-threatening events.

1.2. Implantable Glucose Sensor

The ADA's Consensus Statement on Self-Monitoring of Blood Glucose (SMBG) recommends that diabetic patients should test their blood glucose level at least twice for Type II diabetes and four (for Type I diabetes) times a day [5]. To maintain normal or near normal blood glucose levels (70-120 mg/dL), diabetic patients require injections of insulin, and have to monitor their own blood glucose levels throughout the day. However, the general use of over-the-counter glucose meters requires finger pricking to obtain blood samples several times each day. Because of the high density sensory neurons located in the dermis on the finger tip, patients frequent suffer from painful [6]. Thus, the painfulness, inconvenience, and discomfort of self-monitoring of blood glucose are frequent obstacle to effective patient compliance and optimal management of diabetes.

To corrective regulate tight blood glucose control, a continuous glucose monitoring system (CGMS) is required. The CGMS can provide additional data to track unpredictable glucose trend in relation to meals and exercise [Fig. 1.1] and allow hypoglycemic and hyperglycemic excursions to be avoided. During the past thirty years many kinds of continuous glucose monitoring systems have been studied. These include sensors implanted in the subcutaneous tissue [7-13], sensors implanted in the vascular bed [14,15], and determining glucose concentration in interstitial fluid sampled using a micro dialysis device [16-18]. Although several studies of implantable glucose sensors have been reported, none of the biosensors tested well capable of reliable in continuous blood

3
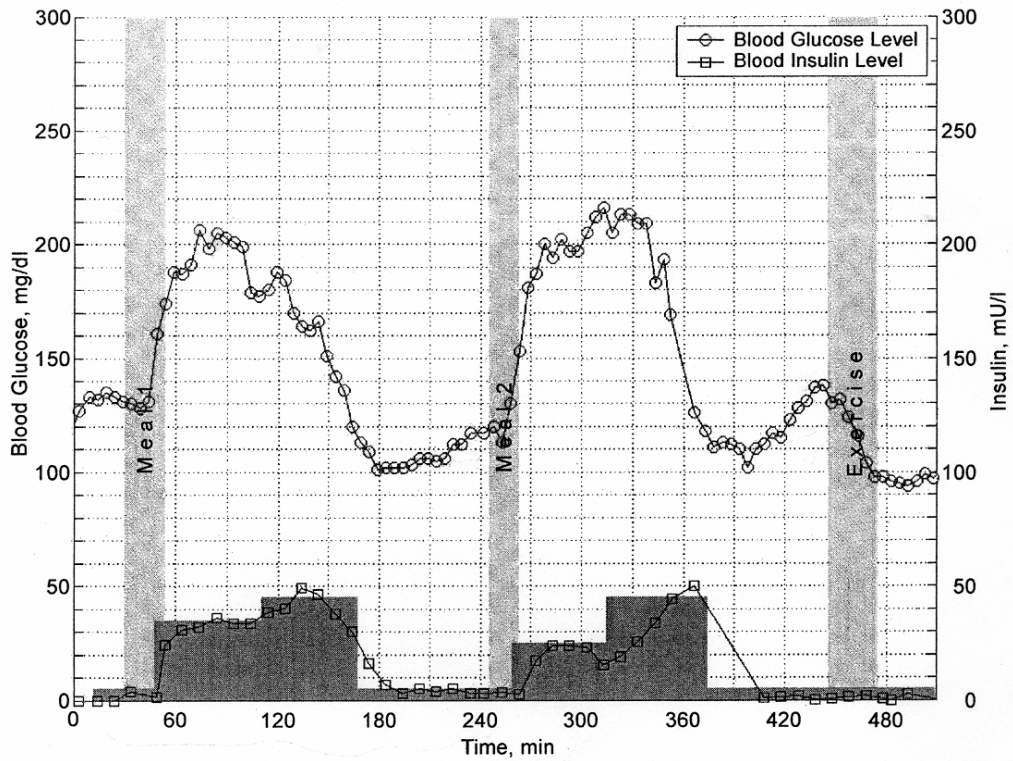
Figure 1.1.   Demonstration of Glucose Rise and Fall in Relation to Meals and Exercise. Figure adapted from Joseph and Torjman [19].

4

glucose monitoring during long-term implantation, progressive loss of sensor function occurred due in part to biofouling and to the consequences of a foreign body response, such as inflammation, fibrosis, and loss of vasculature [20-22].

Most of the implantable glucose sensors are based on amperometric enzyme sensors from the pioneering work of Clark and Lyons [23], Updike and Hicks [24], and Gough et al. [25]. The typical enzyme-based amperometric sensor is composed of a two-electrode system with a glucose indicating platinum (Pt) working electrode and a silver/silver chloride (Ag/AgCl) reference-counter electrode. Figure 1.2 shows the needle-type implantable glucose sensor commonly used for subcutaneous insertion [26]. An outer layer of polyurethane membrane is permeable to glucose and oxygen but impermeable to most interfering substances. A crosslinked glucose oxidase (GOD) enzyme layer is sandwiched between inner and outer membrane. In the presence of oxygen, glucose is oxidized by GOD and produces hydrogen peroxide (H_2O_2). Hydrogen peroxide is then oxidized electrochemically at the Pt electrode surface using a polarization voltage of about +700 mV, producing 2e$^-$ that is detected as a current [21,27]. The chemical reactions are:

$$\text{Glocose} + O_2 \xrightarrow{\;GOD\;} \text{Gluconic Acid} + H_2O_2$$

$$H_2O_2 \xrightarrow{\;+700mV\;} 2e^- + 2H^+ + O_2$$

5
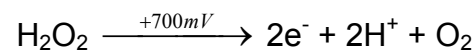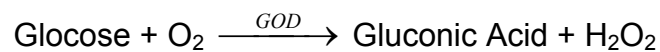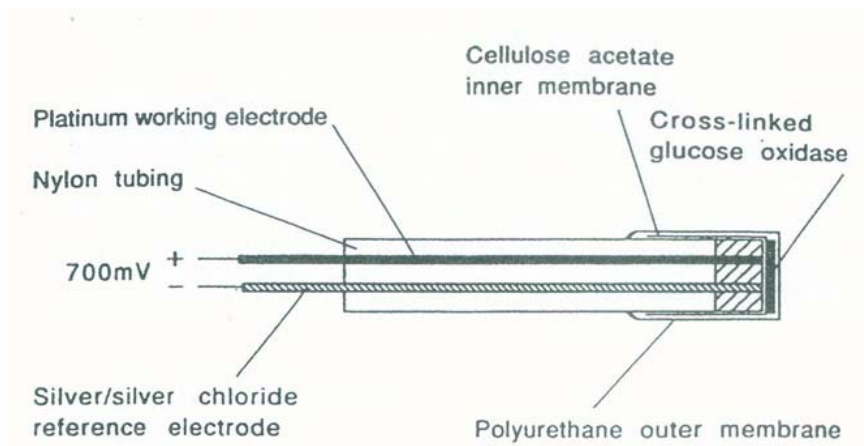
Figure 1.2. Schematic Illustration of the Needle-type Implantable Glucose Sensor.
Figure adapted from Pickup et al. [26].

1.3. Biocompatibility of Implanted Devices

Most implanted medical devices, including biosensors, frequently encounter a sequence of common host defense mechanisms, such as acute and chronic inflammation, wound healing, and foreign body responses [28] [Fig. 1.3]. Acute inflammation begins within a few minutes after device implantation, with accumulation of interstitial fluid, plasma proteins, and migration of leukocytes (neutrophils, monocytes, macrophages) around sensors. Chronic inflammation follows if acute inflammation is not resolved. In general, macrophages rapidly differentiate from monocytes and become the predominant cell type in exudates surrounding the devices. The macrophages are key mediators in the development of immune reactions to implanted synthetic biomaterials. They also produce and secrete a number of biologically active products including chemotactic factors, reactive oxygen metabolites, growth factors, and cytokines [29]. Wound healing is the repair and remodeling process which occurs after. It takes place in the space between the implant and the surrounding tissue. It is begun by the action of monocytes and macrophages, followed by proliferation of fibroblasts and vascular endothelial cells at the wound site. The fibroblasts and new small blood vessels proliferate in developing granulation tissue [28]. The new small blood vessels are budded or sprouted from preexisting blood vessels. This process is called neovascularization or angiogenesis [30-32]. Fibroblasts also synthesize type III collagen and proteoglycans at the wound site. Eventually, collagen deposition may result in the formation of fibrous capsule around the implanted device.

7
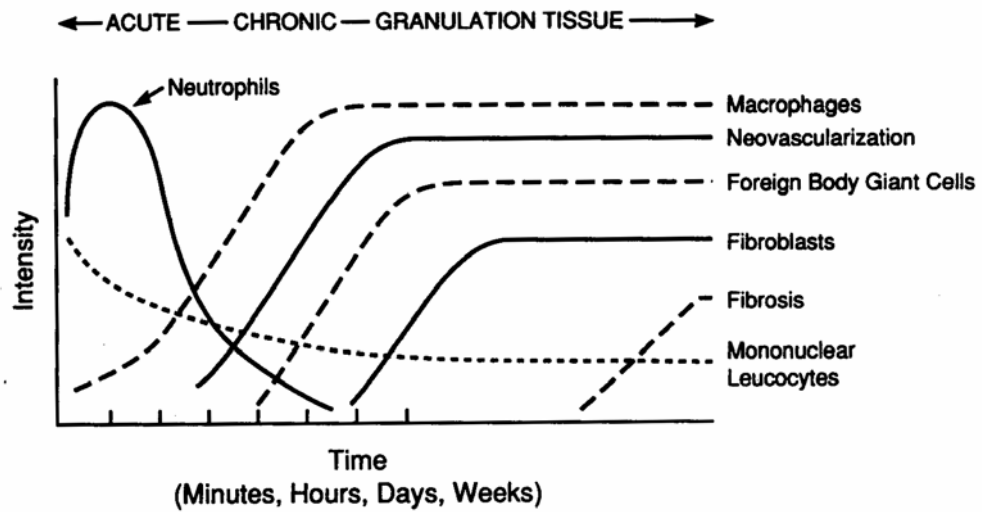
Figure 1.3.   Temporal Variation in Tissue Reaction to Implanted Biomaterials.
                     Figure adapted from Anderson [28].

The foreign body reaction has a connection with foreign body giant cells and granulation tissue including macrophages, fibroblasts and new capillaries at the tissue-implant interface. Fibrosis or fibrous encapsulation is the end-stage of the healing process. Fibrotic tissue surrounding the implanted device isolates it from the local tissue environment. Figure 1.4 shows the process of wound healing in the presence of an implant.

Pore size and pore density on the surface of implanted device (i.e. scaffold) may greatly influence fibrous capsule thickness, blood vessel density, and the location of vessels within the three-dimensional scaffold [19]. Large pore scaffolds (pores > 8 microns in diameter) allow deep penetration of capillaries and supporting extra-cellular matrix (ECM). Sharkawy et al. [33] showed that after four weeks of subcutaneous implantation in rat, well-organized collagen capsule typical of foreign-body responses around non-porous implants, while porous implants produced less fibrosis and more vascularized fibrous capsules.

For implantable biosensors, adsorption of proteins and cells as well as the formation of a fibrous capsule tissue can severely hinder transport of small molecules, i.e. glucose. Glucose is not able to freely diffuse from capillary blood to the sensor's transducer surface [21]. Pickup et al. [26] reported an example of protein and cellular accumulation on the tips of the non-functioned glucose sensors after only five hours of implantation [Fig. 1.5]. Ertefai and Gough [13] showed fibrous capsule tissue surrounding a glucose sensor tip after 10 days of implantation in subcutis [Fig. 1.6].

9

Reichert and Sharkawy [21] reviewed the findings of several implantable biosensor studies:

- Inflammatory cells bind to and degrade sensor performance.

- Protein adsorption hinders sensor function by lowering permeability to glucose and oxygen.

- Fibrous tissue and exogenous pool of foreign body capsule (FBC) presents a transport barrier to glucose.

- Vascularization of the FBC is necessary for good long-term stability of response.

- Sensors inactivated in vivo often regain function when FBC is removed and retested *in vitro*.

- Sensor baseline and sensitivity gradually degrade with implantation time.

- Sensor performance is erratic for the first hour and then becomes steady upon equilibration.

- Subcutaneous (SQ) glucose levels lag behind plasma levels by 5-20 min.

- Intravascular (IV) implantation gives immediate glucose readings but suffers from thrombus formation.

- IV implantation is best if the sensor is placed in fast-moving blood stream.

- Intraperitoneal (IP) FBC is thinner than SQ.

- Textured coatings produce vascularized FBC that might ensure long-term SQ sensor accuracy.
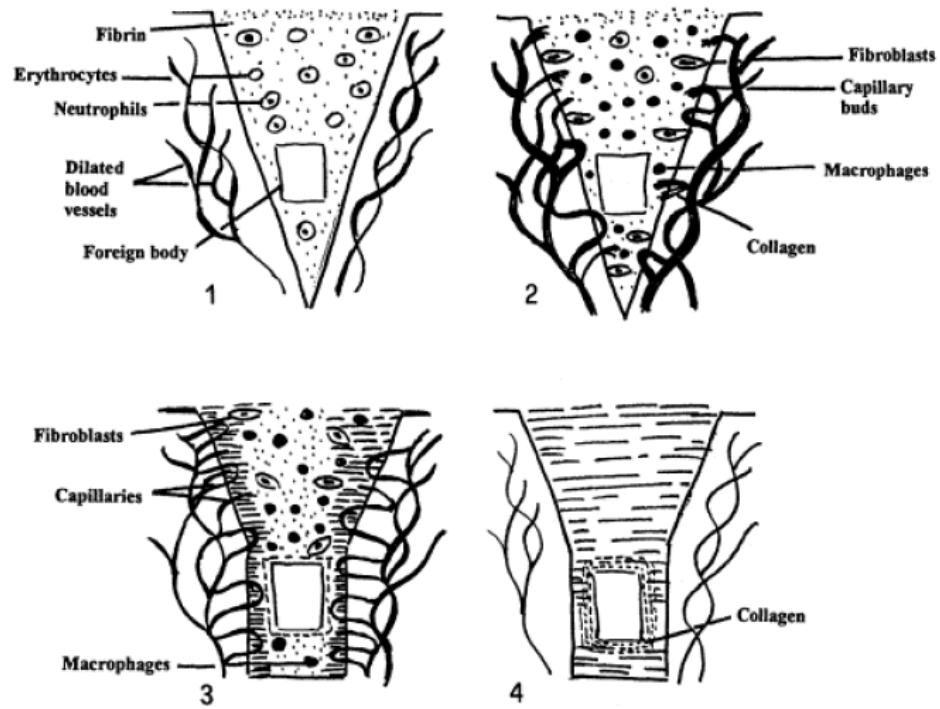
Figure 1.4. Schematic of Process of Wound Healing in the Presence of an Implant. Figure adapted from Cannas et al. [34].
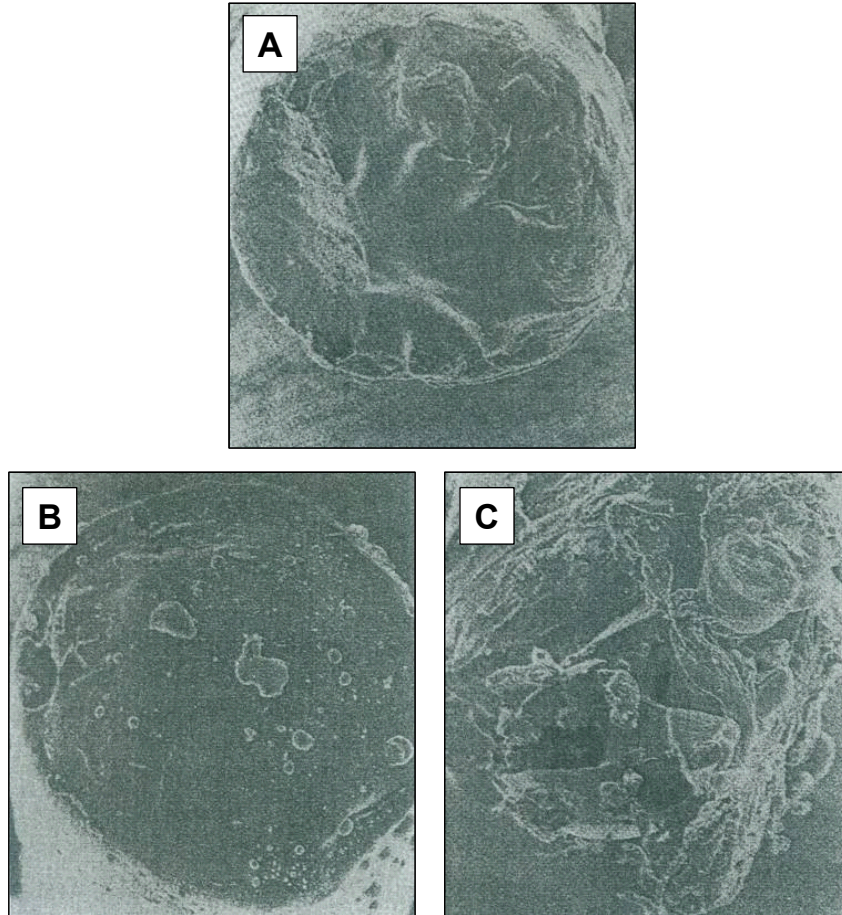
Figure 1.5.   SEM Photographs of Tips of Glucose Sensors. (A) Control sensornot implanted; (B) Functioning sensor showing minimal biofouling;   (C) Non-functioning sensor showing significant protein and Cellular accumulation. Figure adapted from Pickup et al. [26].
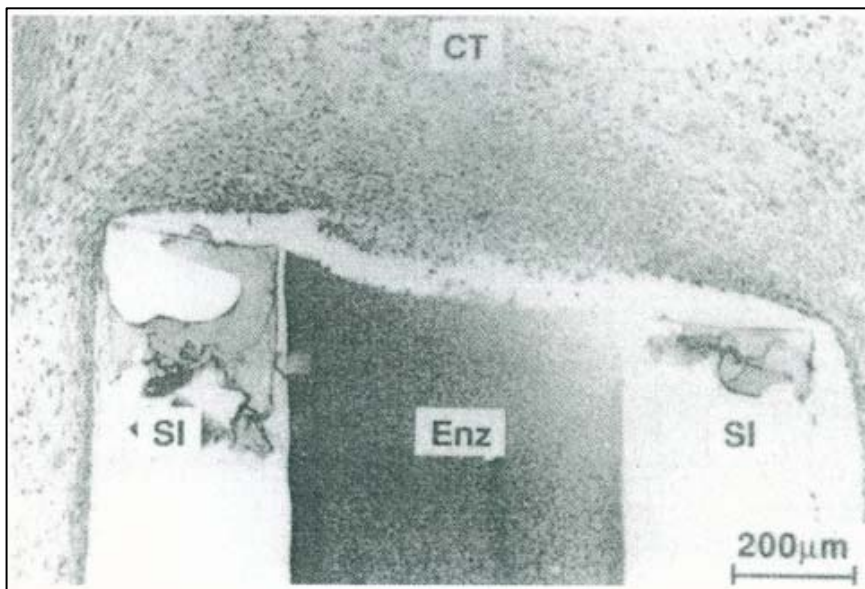
Figure 1.6.   Light Micrograph Image of Glucose Sensor Tip after 10 Days of Implantation in Subcutis. Note dense fibrous capsule surrounds sensor. Figure adapted from Pickup et al. [13].

13

1.4. Strategies for Biocompatible Implantable Sensors

Many researchers studied sensor modification to reduce sensor membrane biofouling *in vivo*. One approach is to reduce protein adsorption. Quinn et al. [35] used poly(ethylene glycol) (PEG) into a poly(hydroxyethyl-methacrylate) (PHEMA) for surface modification of the biosensor. The PEG chains tend to stand perpendicular to the membrane surface to provide a water rich phase that resists many protein molecules. Vadgama et al. [36,37] tried to reduce protein adsorption by using diamond-like carbon, so-called "inert" materials. Shichiri et al. [38] incorporated an alginate/polylysine gel layer on the sensor. Shaw et al. [39] reported biocompatibility improvement of biosensor, coated with PHEMA/polyurethane (PU). Wilkins et al. [40] and Moussy et al. [7,41-43] introduced the Nafion^{TM} (perfluorosulphonic acid) membrane, to reduce biofouling on surface of the sensor and reduce interference from urate and ascorbate. Armour et al. [14] coated their sensor tips with crosslinked albumin and Kerner et al. [44] developed cellulose-coated sensors to improve sensor blood compatibility.

Controlled delivery of tissue response modifiers (TRM) can be used to control tissue responses. Dexamethasone (Dex), a synthetic glucocorticoid, is well known for its immunosuppressive and anti-inflammatory function [45-47]. The biosensor design could incorporate this anti-inflammatory agent, which could be slowly released using biodegradable microspheres [48,49]. Typically, microspheres are prepared using natural or synthetic biodegradable polymers such as poly(lactic-co-glycolic acid) (PLGA) [49]. Moussy et al. [50,51] developed

14

Dex/PLGA microspheres designed to suppress the inflammatory tissue response to an implanted biosensor. Norton et al. [52] and Patil et al. [53] modified hydrogel coatings [PHEMA and poly(vinyl alcohol) (PVA) hydrogel, respectively] to include Dex-loaded PLGA microspheres to improve implantable biosensor biocompatibility.

The best tissue environment for an implantable biosensor is vascularized tissue around sensor. Angiogenesis, which include as complex cascade of events involving endothelial cell activation, migration and proliferation, organization into immature vessels, association of mural cells with the immature vessels, and matrix deposition as the vessels mature [54,55], has been extensively studied. The control of neovascularization has recently focused on the use of angiogenic growth factors such as vascular endothelial growth factor (VEGF) and platelet-derived growth factor (PDGF). VEGF is a specific mitogen for initiating angiogenesis, specifically, for promoting vascular permeability, prolifieration, and migration of endothelial cells [56]. PDGF promotes the maturation of blood vessels by the recruitment of smooth muscle cells to the endothelium lining of nascent vasculature [55,57].

The controlled release of VEGF and PDGF has been studied widely as a strategy for increasing the blood vessel density surrounding implants [58-61]. Klueh et al. [62,63] developed an *in vivo* gene transfer system with VEGF and found that the VEGF-biosensor systems induced neovascularization surrounding the sensor and thereby enhanced biosensor function *in vivo*. Ward et al. [64] reported that VEGF infused continuously for 28 days into rat subcutaneous tissue

15

from a model biosensor led to local vascularization of the surrounding foreign body capsule. Norton et al. [52] modified their hydrogel biosensor coatings to incorporate PLGA microspheres in order to release vascular endothelial growth factor.

16

1.5. Collagen and Its Use in Biomaterials

In recent years, collagen and its derived matrices have become the most widely used natural polymers in the biomedical field including tissue engineering due to their low antigenicity, biodegradability and good mechanical, hemostatic and cell-binding properties [65-69]. A broad range of potentially manufactured products based on collagen is covering many medical disciplines [70] (Table 1).

Collagen is a major protein of connective tissues in animals as well as a key structural component of the extracelluar matrix. It is distributed in skin, bones, teeth, tendons, eyes and most other tissues and organs [71,72]. The collagen molecule is a rod-like structure with a molecular weight of about 300,000 which forms a unique triple-helix configuration of three polypeptide subunits. Each collagen molecule is organized in a regular and hierarchical pattern forming fibrils and fibril bundles that result in a tough tissue [73,74]. The collagen family has been reported to contain at least 19 distinct types. Among them, type I collagen is the most abundant in higher order animals in the skin, tendon, bone, and most collagenous tissue, while type II is found in cartilage, and type III is found, together with type I, in skin, and blood vessels. Thus, type I collagen is predominantly encountered in biomaterials application as bioprosthetic devices and scaffolds [71,73].

In order to devise strategies for using collagen in the development of advanced biomaterials for biomedical engineering, it is necessary to confer mechanical strength and enzymatic degradation (e.g. collagenase) resistance by introduction of chemical or physical crosslinking into the molecular structure.

17

Table 1.1. Examples of Applications of Collagen-Based Medical Devices [71].

Medical Area	Application
Cardiovascular surgery	Vessel replacement, heart valves
Dentistry	Periodontal attachment, alveolar ridge augmentation
Dermatology	Tissue augmentation
General surgery	Hernia repair, adhesion barriers, tissue adhesives
Neurosurgery	Nerve conduits, nerve repair
Ophthalmology	Corneal graft, vitreous replacement
Orthopedics	Bone repair, cartilage and ligament reconstruction
Otology	Tympanic membrane replacement
Urology	Ureter replacement, renal repair, urinary incontinence
Wound management	Dressings

There are several methods for crosslinking collagen-based biomaterials. Glutaraldehyde (GA) is the most widely used as a crosslinking agent for collagen-based biomaterials [65,75]. At neutral pH, GA reacts with amino groups and with other functional group in protein, including carboxy and amide group [76]. However, GA induces cytotoxicity in vivo, caused by the presence of unreacted residual groups or the release of monomers of small polymers during enzymatic degradation [77,78]. To avoid cytotoxicity and calcification of GA-crosslinked collagen, polyepoxy compounds, including glycol and glycerol polyglycidyl ethers, have been examined as potential collagen crosslinking agents [79,80]. Polyepoxy compounds react with the free amines of lysine side chains on neighboring proteins. The hexamethylene diisocyanate (HMDI), homobifunctional reagent, has the ability to crosslink collagen via its lysine side chains. Chvapil et al. [81,82] reported that HMDI is an effective method for crosslinking of collagen and does not leave residues after crosslinking process. Crosslinking with carbodiimide, 1-ethyl-3-(3- dimethylaminopropyl) carbodiimide (EDC) and *N*-hydroxysuccinimide (NHS) being the most widely used as crosslinking agents, has the main advantage in that it only facilitates the formation of amide bonds between amino group on the collagen molecules without becoming part of the actual linkage [73]. This method provides good biocompatibility and higher cellular differentiation potential [66,83,84]. Koob et al. [85-88] has newly developed a process for polymerizing type I collagen fibers with nordihydroguaiaretic acid (NDGA), a plant-derived compound. NDGA crosslinking is effective at significantly improving the mechanical properties of

19

synthetic collagen fibers. Also, NDGA- crosslinked collagen fibers did not elicit a foreign body response nor did they stimulate an immune reaction *in vivo* during a six week implantation period. In addition, various physical treatments including ultra-violet or gamma-ray irradiation, and dehydrothermal treatment, have been effectively used for introducing crosslinks to collagen matrices [89-92].

CHAPTER 2

IN VITRO / IN VIVO STABILITY OF THE SCAFFOLDS AND *IN VITRO* SENSITIVITY OF IMPLANTABLE GLUCOSE SENSORS WITH SCAFFOLDS

2.1. Introduction

To maintain near normal blood glucose levels (70-120 mg/dL), diabetic patients widely use over-the-counter glucose meters, which require finger pricking to obtain blood samples several times a day. The pain [6], inconvenience, and discomfort of self-monitoring of blood glucose (SMBG) are frequently obstacles to effective patient compliance and optimal management of diabetes. During the past 20 years many kinds of continuous glucose monitoring systems have been studied including sensors implanted in the subcutaneous tissue [7-13], sensors implanted in the vascular bed [14,15], and determining glucose concentration in interstitial fluid sampled using a micro dialysis device [16-18]. Although several studies of implantable glucose sensors have been reported, none of these biosensors are capable of continuously monitoring glucose levels during long-term implantation reliably. Progressive loss of sensor function occurs due in part to biofouling and to the consequences of a foreign body response such as inflammation, fibrosis, and loss of vasculature [20-22].

21

Many researchers have modified the surface of the sensors to reduce membrane biofouling *in vivo*. In an approach to reduce protein adsorption, Quinn et al. [35] used poly(ethylene glycol) (PEG) in a polyhydroxyethylmethacrylate (PHEMA)matrix. Since the PEG chains tend to stand up perpendicular to the membrane surface, they provide a water-rich phase that resists binding of many protein molecules. Vadgama's et al. [36,37] reduced protein adsorption by using diamond-like carbon, so-called "inert" materials. Shichiri et al. [38] incorporated an alginate/polylysine gel layer at the sensor. Shaw et al. [39] reported improvement in biocompatibility of a biosensor coated with PHEMA/PU (polyurethane). Wilkins et al. [40] and Moussy et al. [7,41-43] introduced Nafion[TM] (perfluorosulphonic acid) membrane, to reduce "biofouling" on the surface of the sensor and reduce interference from urate and ascorbate. Armour et al. [14] coated their sensor tips with crosslinked albumin and Kerner et al. [44] developed cellulose-coated sensors to improve sensor blood compatibility. However, none of these approaches has been successful for long term, stable glucose monitoring.

Collagen and its derived matrices are used extensively as natural polymers in the biomedical field including tissue engineering due to its low antigenicity, its biodegradability and its good mechanical, haemostatic and cell-binding properties [65-69]. In order to devise strategies for using collagen in the development of advanced biomaterials for biomedical engineering, it is necessary to confer mechanical strength and resistance to enzymatic (collagenase) degradation resistance with chemical or physical crosslinking

22

strategies. There are several strategies for crosslinking collagen-based biomaterials. Glutaraldehyde (GA) is the most widely used as a crosslinking agent for collagen-based biomaterials [65,75]. However, GA and its reaction products are associated with cytotoxicity *in vivo*, due to the presence of crosslinking byproducts and the release of GA-linked collagen peptides during enzymatic degradation [77,78].

To avoid *in vivo* cytotoxicity and subsequent calcification of GA-crosslinked collagen, several alternative compounds have been examined as potential collagen crosslinking agents [79,80] such as polyepoxy, hexamethylene diisocyanate (HMDI), 1-ethyl-3-(3-dimethylamino-propyl)carbodiimide (EDC), and ultra-violet (UV) or gamma-ray irradiation. Koob et al. [85-88] recently described a process for crosslinking of type I collagen fibers with nordihydroguaiaretic acid (NDGA), a plant compound with antioxidant properties. They showed that NDGA significantly improved the mechanical properties of synthetic collagen fibers. In addition, they showed that NDGA-crosslinked collagen fibers did not elicit a foreign body response nor did they stimulate an immune reaction during six weeks *in vivo*.

The extent of crosslinking and choice of crosslinking agent may also affect the porosity and pore size of the scaffold and may greatly influence fibrous capsule thickness, blood vessel density, and the location of vessels within the three-dimensional porous scaffold [19]. Large pore scaffolds (greater than 60 micron pore size) allow deep penetration of capillaries and supporting extracellular matrix (ECM). Sharkawy et al. [33] recently showed that after four

23

weeks of subcutaneous implantation in rat, a well-organized collagen matrix typical of a foreign-body response encapsulated non-porous implants, while the porous polyvinyl alcohol (PVA) implants produced less fibrous and vascularized tissue capsules.

The goal of this study was to develop a new porous collagen scaffold around implantable glucose sensors for improving their biocompatibility. We fabricated porous collagen scaffolds by using a freeze-drying method followed by crosslinking using NDGA or GA. We evaluated the resistance of NDGA- and GA-crosslinked collagen scaffolds to degradation using both *in vitro* and *in vivo* experiments. We also applied the scaffolds around a coil-type implantable glucose sensor and measured sensor function *in vitro*.

2.2. Materials and Methods

2.2.1. Materials

Type I collagen (purified from fetal bovine tendon) was a generous gift from Shriners Hospital for Children (Tampa, FL). Nordihydroguaiaretic acid (NDGA) was purchased from Cayman Chemical Co. (Ann Arbor, MI). Glucose, bovine serum albumin (BSA) and 50% (w/w) glutaraldehyde (GA) were obtained from Fisher Scientific (Pittsburgh, PA). Glucose oxidase (GOD) (EC 1.1.3.4., type X-S, *Aspergillus niger*, 157,500 U/g), epoxy adhesive (ATACS 5104), polyurethane (PU), tetrahydrofuran (THF) and collagenase (EC 3.4.24.3, type I, from *Clostridium histolyticum*, 302 U/mg) were obtained from Sigma-Aldrich (St. Louis, MO). Sprague-Dawley out-bred rats (male, 375-399 g) were purchased from Harlan (Dublin, VA).

2.2.2. Preparation and Crosslinking of Collagen Scaffolds

The collagen scaffolds were prepared by a freeze-drying method. Collagen was dissolved in 3% acetic acid to prepare a 1% (w/v) solution. The solution was applied to a cylinder-shaped polypropylene mold (Φ 10 mm, height 8 mm) and then freeze-dried. A cylindrical 3D porous scaffold was obtained. The scaffolds were then crosslinked with NDGA or GA to minimize solubility and improve resistance to collagenase degradation.

For NDGA crosslinking, dried collagen scaffolds were briefly soaked in absolute ethanol, followed by soaking in 2 M of NaCl solution for 12 h at room temperature. Scaffolds were re-suspended in oxygen sparged phosphate

buffered saline (PBS, 0.1 M NaH$_2$PO$_4$, pH 9.0) for 30 min. at room temperature. Scaffolds were then treated with 3 mg of NDGA in 1 mL of PBS as follow: NDGA was dissolved in 0.4 N NaOH at a concentration of 30 mg/mL. One milliliter of the NDGA solution was added directly to PBS in which the scaffolds were suspended to a final concentration of 3 mg/mL. The scaffolds were agitated in the NDGA solution for 24 h at room temperature. The scaffolds were removed, briefly rinsed with water and freeze-dried.

For a comparative study of the effectiveness of the NDGA treatment, other scaffolds were treated with 0.5% GA for 2 h or 12 h in ethanol solution at room temperature. To prevent the dissolution or loss of the matrix during the GA crosslinking process, we used 100% ethanol instead of water. The crosslinked scaffolds were washed with de-ionized water and freeze-dried again. The morphology of the scaffolds before/after crosslinking was examined using scanning electron microscopy (SEM) after gold sputter coating of the samples in a metal evaporator according to standard procedures.

To evaluate the stability of the scaffold after crosslinking, the degree of crosslinking (Dc) was estimated by weighing the dried samples before and after crosslinking. Dc was calculated using the following equation:

Dc [%] = (sample mass after crosslinking /

sample mass before crosslinking) × 100

The swelling property of the porous scaffolds was examined by measuring water absorption. The scaffolds were weighed after thorough drying (W_{dry}) and immersed in purified water. After 24 h, the scaffolds were removed from the water and immediately weighed again (W_{wet}). Water absorption was calculated by using the following equation:

$$\text{Water absorption (\%)} = [(W_{wet} - W_{dry})/W_{wet}] \times 100$$

2.2.3. *In vitro* and *In vivo* Evaluation of Collagen Scaffolds

To examine the biological stability of the crosslinked scaffolds, we performed *in vitro* and *in vivo* biodegradation tests. *In vitro* biodegradation of NDGA- and GA-crosslinked scaffolds was tested using bacterial collagenase. Fabricated NDGA- and GA-crosslinked collagen scaffolds were incubated in the collagenase solution (1 mg/mL in PBS at 37°C) for up to 4 weeks. Scaffolds were removed from the solution, rinsed with de-ionized water and freeze-dried at given time intervals (weeks 1 to 4) during incubation. The *in vitro* degradation was evaluated as the percentage of weight difference of the dried scaffold before and after enzyme digestion.

To determine the stability of the crosslinked scaffolds *in vivo*, we directly implanted NDGA- and GA-crosslinked collagen scaffolds in rats. The scaffolds were disinfected with 70% ethanol solution for 2 h and implanted subcutaneously in the back of the rats. Scaffolds were explanted at 7, 14, 21, and 28 days after implantation. After explantation, the scaffolds were examined macroscopically.

27

2.2.4. Preparation of Porous Collagen Scaffolds around Implantable Glucose Sensors

We first fabricated coil-type glucose sensors loaded with crosslinked enzyme (GOD: Glucose Oxidase) using a Platinum-Iridium (Pt/Ir) wire (Teflon coated, Φ 0.125 mm, Pt:Ir = 9:1, Medwire, Sigmund Cohn Corp.). Then, we applied bovine tendon type I collagen scaffolds around the sensors [Fig. 2.1]. Briefly, in order to fabricate a glucose sensor, the Teflon coating of the top 10 mm of a Pt/Ir wire was removed and the wire was wound up along a 30-gauge needle to form a coil-like cylinder. The cylinder unit had an outer diameter of 0.55 mm and an inner diameter of 0.3 mm and a length of 1 mm. A cotton thread was inserted inside the coil chamber to retain the enzyme solution during enzyme coating of the electrodes. GOD was added and crosslinked to the sensors by dip coating in an aqueous solution containing 1% GOD, 4% BSA, and 0.6% (w/w) glutaraldehyde. The outer membrane of the sensor was coated with Epoxy-Polyurethane (Epoxy-PU) by dipping in Epoxy-PU solution (2.5% (w/v) in THF, Epoxy:PU = 1:1). The sensor was dried at room temperature for at least 24 h. The two ends of the sensing element were sealed by electrically-insulating sealant (Brush-On electrical tape, North American Oil Company) [93,94].

To apply collagen scaffolds around the sensors, the sensors were dip-coated with 1% (w/v) collagen solution and freeze-dried. The porous scaffolds around the glucose sensors were crosslinked with either NDGA or GA as previously described. Obtained sensors were stored dry at room temperature or

28
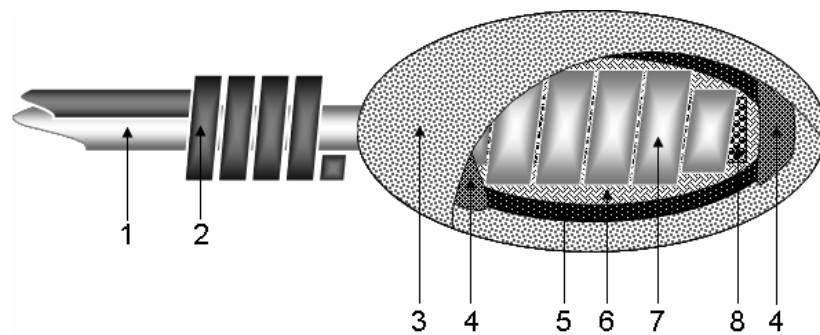
Figure 2.1. Schematic Diagram of the Scaffold-coated Sensing Element of the
Glucose Electrode.
(1) Teflon-covered Pt-Ir wire;
(2) Ag/AgCl reference wire;
(3) Collagen scaffold;
(4) Electrically-insulating sealant;
(5) Epoxy-Pu outer membrane;
(6) Enzyme layer;
(7) Stripped and coiled Pt-Ir wire;
(8) Cotton fiber with GOD gel.

29

in PBS at 4°C. The morphology of the sensors was observed using light microscope and SEM. In addition, in order to evaluate sensitivity changes of the sensors with varying wall thickness of the scaffold around the sensors, we controlled the wall thickness of the scaffold by multiple dipping /freezing cycles in collagen solution. The scaffold with the sensor was then freeze-dried and crosslinked as previously described.

Silver wires (Teflon coated, Φ 0.125 mm, World Precision Instruments, Inc.) were used to fabricate the Ag/AgCl reference electrodes. Silver wires were coiled and anodized galvanostatically at 1mA overnight in stirred 0.1 M HCl [93,94].

2.2.5. *In vitro* Characterization of Sensors Coated with Scaffolds

The glucose sensors were characterized in PBS (pH 7.4) at 700 mV versus the incorporated Ag/AgCl reference electrodes. The working electrode (Pt/Ir wire) and Ag/AgCl reference electrode of each sensor were connected to an Apollo 4000 potentiostat (World Precision Instruments, Inc.). The background current was allowed to stabilize for 10 min., and the sensors were then exposed to a series of glucose solutions in order to examine their sensitivities and linearities. The response sensitivity (S) was repeatedly assessed by 1) measuring the response current (I_1) of a C_1 glucose solution, 2) adding a concentrated glucose solution into the measured solution to increase the glucose concentration to C_2, and 3) measuring the response current (I_2) of the resulting

www.manaraa.com

solution. The sensitivity was expressed as the current increase caused by a 1 mM glucose increase, i.e. $S = (I_2 - I_1) / (C_2 - C_1)$.

2.3. Results and Discussion

2.3.1. Preparation of Porous Crosslinked Collagen Scaffolds

The chemistry of the NDGA crosslinking reaction differs from the reaction using the GA treatment [Fig. 2.2]. GA is the most common crosslinking agent used for fixation of collagen scaffolds for tissue bioengineering. Both aldehyde functional groups of the GA molecule react with amine groups between two neighboring polypeptide chains, particularly lysine side chains. Unfortunately, GA crosslinking is encumbered with potential cytotoxicity problems caused by the presence of unreacted residual groups or the release of monomers and small polymers during enzymatic degradation [77,78].

NDGA treatment is an alternative crosslinking agent, which possesses reactive catechols. Collagen crosslinking with NDGA mimics the quinine tanning mechanism in the skate egg capsule. Catechol-quinone tanning systems are prevalent in a wide variety of animals, which the process serves to strengthen vulnerable extracellular matrices (e.g. insect cuticle, mussel byssus threads) [85,95]. NDGA, isolated from the creosote bush, is a low molecular weight di-catechol containing two *ortho*-catechols. The two catechols on NDGA undergo auto-oxidation at neutral or alkaline pH producing reactive quinones. Two quinones then couple via aryloxy free radical formation and oxidative coupling, forming bisquinone crosslinks at each end. The NDGA continues forming a large crosslinked bisquinone polymer network in which the collagen fibrils are embedded. The NDGA treatment does not form crosslinks with amino acid side chains of collagen [85,86,95].

32

In this study, highly porous collagen scaffolds were prepared by a freeze-drying method. We ascertained that the obtained scaffolds have an open cell and interconnected pore structure based on SEM observation [Fig. 2.3(A)]. The pores of the scaffolds are regularly distributed and range from 20 to 100 µm in diameter (mean ~ 60 µm). Sharkawy et al. [33] reported that the a 60 µm mean-pore-sized polyvinyl alcohol (PVA) sponge provided a tissue in-growth environment and allows to infiltration of neovasculature but did not allow for fibrous tissue in-growth. After crosslinking with NDGA and GA, the pore size and pore structure of both scaffolds were not significantly altered [Fig. 2.3(B) and (C)].

Figure 2.4 shows the degree of crosslinking and water absorption of the scaffolds using different crosslinking methods. The mass was reduced to about 70% after NDGA treatment and 60% for GA treatment after the crosslinking process due to the loss of uncrosslinked collagen components. Crosslinked collagen scaffolds had significantly higher form stability than uncrosslinked collagen scaffolds. Also, the swelling behavior of NDGA- and GA-crosslinked scaffolds showed no significant differences between the two different crosslinking agents. The water absorptions of both crosslinked scaffolds were above 99%. The high swelling property of sponge-like matrices seems to be dependent on the porous inner structure of the scaffold, which possesses good absorbent characteristics [96].
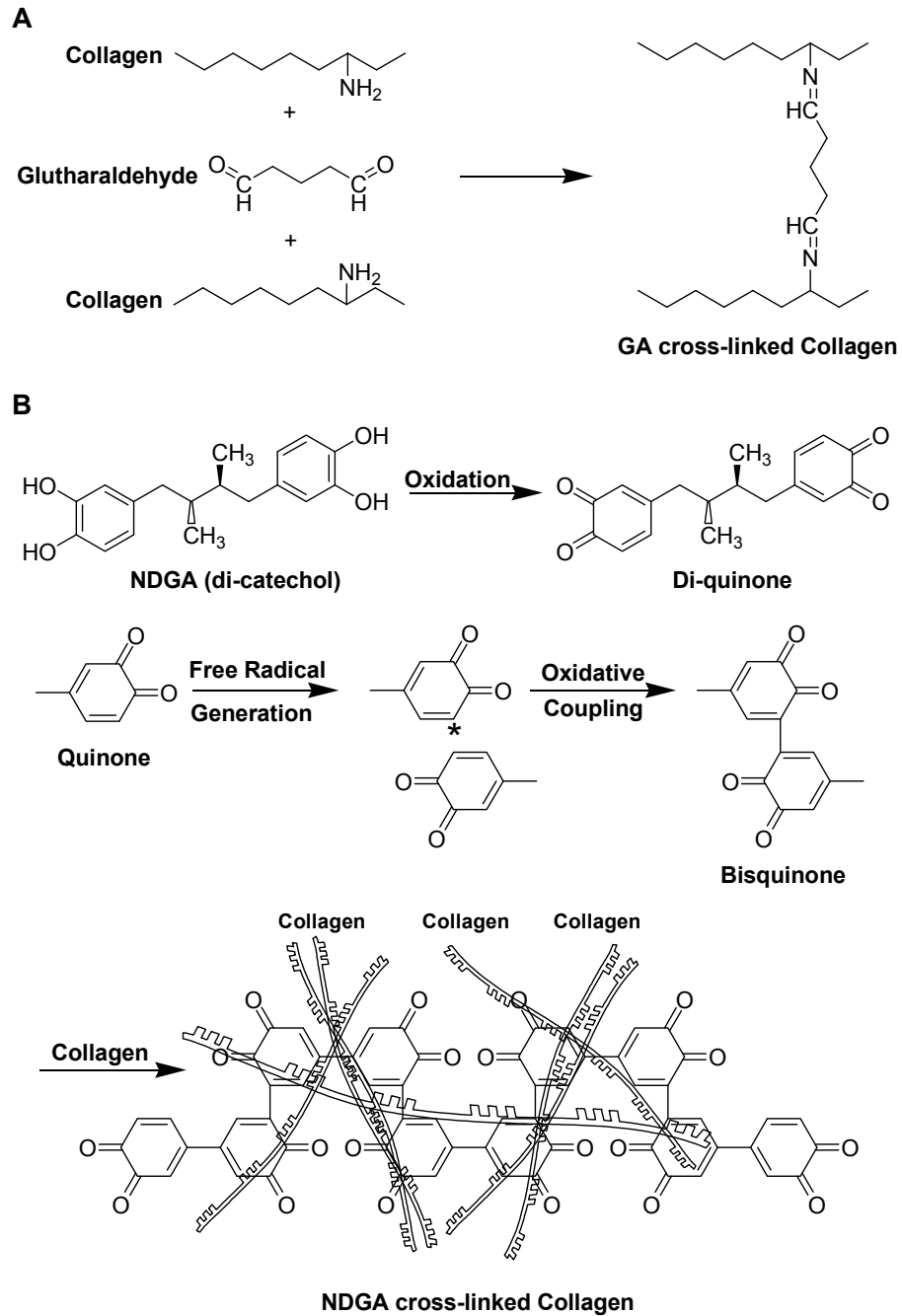
Figure 2.2.   Schematic Mechanism for (A) GA and (B) NDGA Crosslinking of the Collagen Scaffold.

34
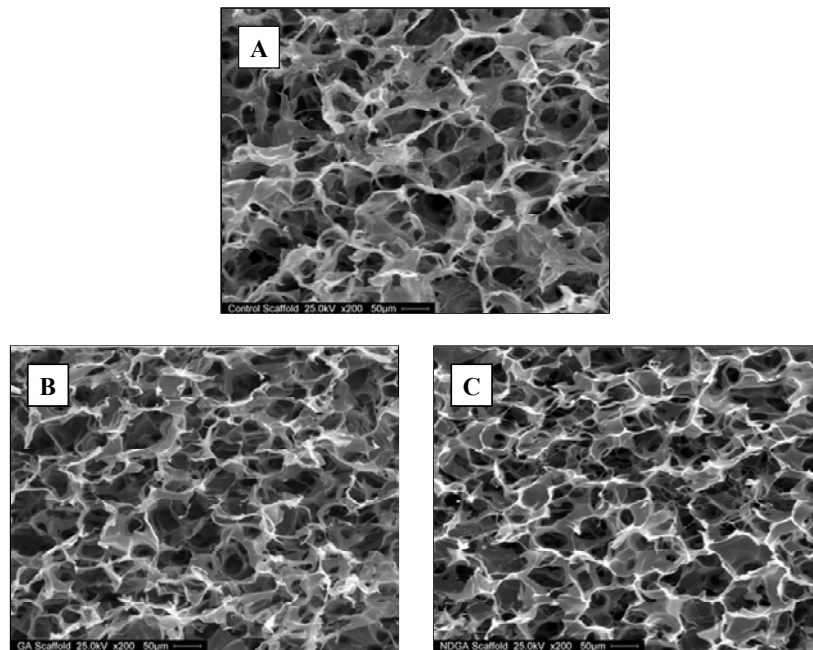
Figure 2.3.   SEM Morphology of the Collagen Scaffold. Determination of the pore size of collagen scaffolds by SEM. (A) No crosslinking; (B) GA-crosslinked; (C) NDGA-crosslinked.

35
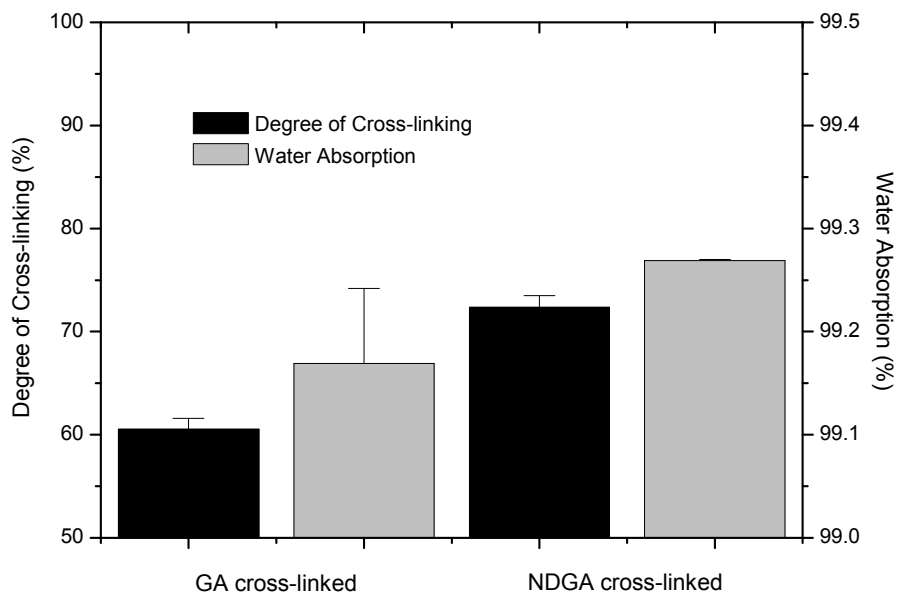
Figure 2.4. Bulk Properties of GA- and NDGA-crosslinked Scaffold.
Results are shown as means ± SD (n=3).

36

www.manaraa.com

2.3.2. *In vitro* and *In vivo* Evaluation of Collagen Scaffolds

The biological stability of the crosslinked collagen scaffolds was investigated by *in vitro* and *in vivo* biodegradation tests. Degradation in both uncrosslinked (control) and crosslinked scaffolds was characterized by determining weight loss of the scaffold after enzymatic digestion. The uncrosslinked scaffolds and scaffolds crosslinked with GA for 2 hours were completely degraded in the collagenase solution within several hours while NDGA- or GA-crosslinked (for 12 h) scaffolds were not degraded within 24 hours. A significant increase in resistance to enzymatic digestion could be shown after crosslinking. Figure 2.5 shows long-term collagenase *in vitro* degradation test (weight remaining %) of the NDGA- and GA-crosslinked scaffolds. After 1 week exposure to collagenase, both types of scaffolds showed high resistance to enzymatic digestion (> 80% weight remaining). After 3 and 4 weeks, all scaffolds retained 70% of their initial mass. However, in the case of GA-crosslinked scaffold, the pore size was increased after 4 weeks collagenase digestion process [Fig. 2.6(B) *vs* Fig 2.6(D)]. In contrast, the pore size of NDGA-crosslinked scaffolds did not appear to increase [Fig. 2.6(A,C)]. As a result, we suggest that NDGA or GA treatment can provide collagen scaffolds with improved enzymatic biodegradation stability. The collagenase cleavage sites were more effectively blocked by the crosslinking of the collagen scaffolds [97].

To study the stability of the crosslinked scaffolds *in vivo*, we implanted crosslinked collagen scaffolds in the subcutaneous tissue of the Sprague-Dawley

37
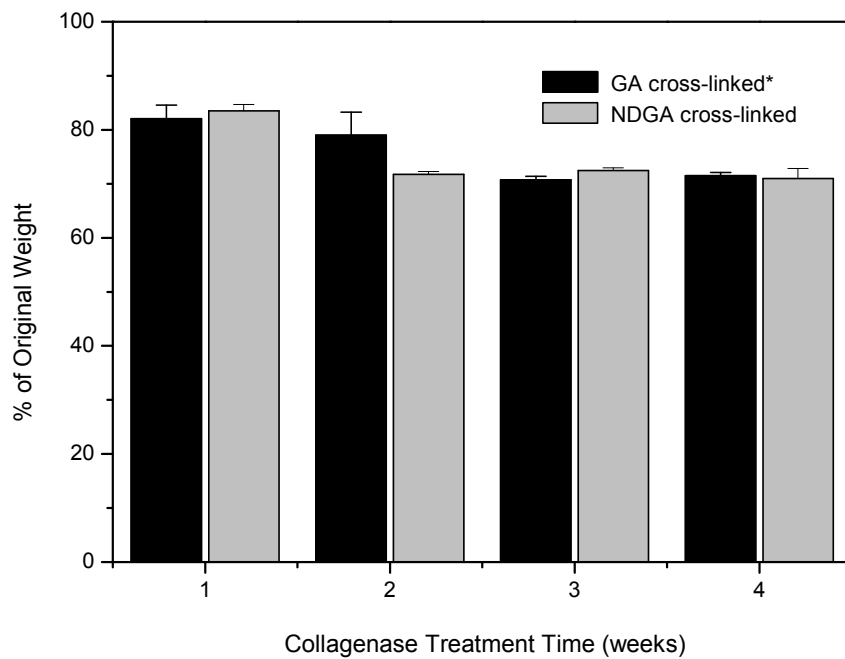
Figure 2.5.   Collagenase Resistance of GA- and NDGA-crosslinked Scaffold *In vitro*. Results are shown as means ± SD (n=3). * Scaffolds were treated with 0.5% GA for 12 h in ethanol solution at room temperature.
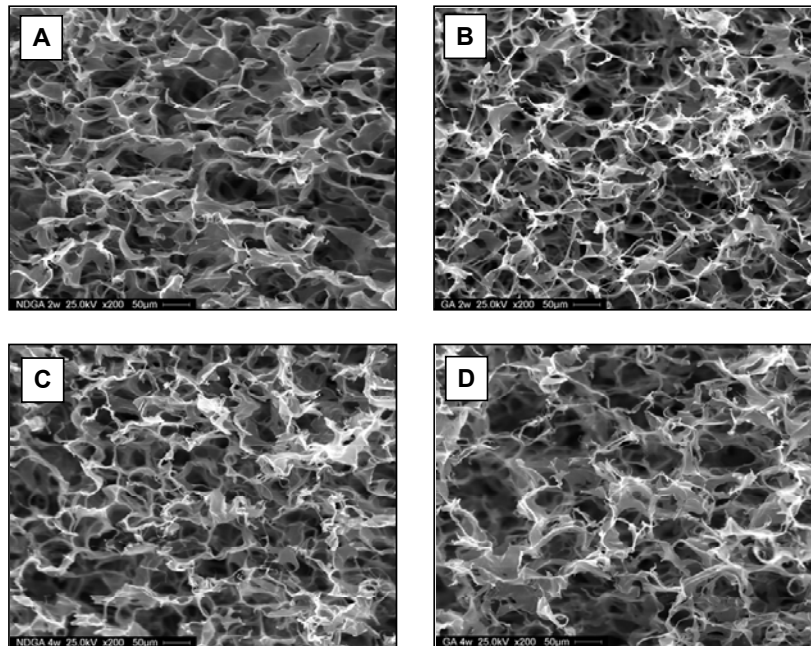
Figure 2.6.   SEM Morphology of the Scaffold after *In vitro* Degradation Study. Results are shown as means ± SD (n=3). (A) NDGA-crosslinked scaffold after 2 weeks collagenase treatment; (B) GA-crosslinked scaffold after 2 weeks collagenase treatment; (C) NDGA-crosslinked scaffold after 4 weeks collagenase treatment; (D) GA-crosslinked scaffold after 4 weeks collagenase treatment.

rats and explanted samples two and four weeks post implantation. After 2 weeks implantation, the NDGA-crosslinked scaffolds did not show evidence of degradation, but the overall shape of the GA-crosslinked scaffolds was deformed and the size slightly reduced because of starting degradation [Fig. 2.7 (A)]. After 4 weeks, the size and shape of the GA-crosslinked scaffolds were dramatically changed (-78% in size of 2 weeks)but there was a small change in the NDGA-crosslinked scaffolds (-18.9% in size of 2 weeks) [Fig. 2.7(B)]. This indicated that the scaffolds treated with the NDGA were more stable than the scaffolds crosslinked with the GA treatment used in these studies.

2.3.3. Porous Collagen Scaffolds around Implantable Glucose Sensors

We first fabricated coil-type glucose sensors loaded with crosslinked enzyme (GOD: Glucose Oxidase) by using Platinum-Iridium (Pt/Ir) wires. Then, we applied bovine tendon type I collagen scaffolds around the sensors [Fig. 2.1]. Yu et al. [94] previously reported that this "coil-type" sensor allows more GOD loading, provides a larger electrochemical surface area, and therefore increases the response current as compared to a "needle-type" sensor. Our sensor is flexible and miniaturized (0.5 mm dia.) for subcutaneous implantation. It is composed of a two-electrode system with a glucose indicating platinum electrode and a Ag/AgCl reference-counter electrode. Our sensor utilizes a three-layer membrane configuration of crosslinked collagen scaffold, epoxy-polyurethane (Epoxy-PU) and GOD. The collagen scaffold (the outer layer in this case) can
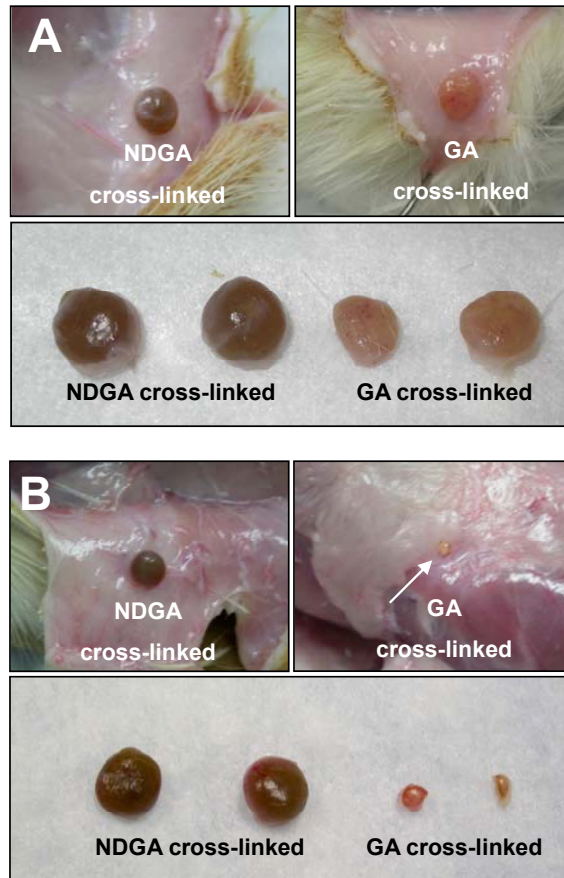
Figure 2.7. *In vivo* Stability of GA- and NDGA-crosslinked Scaffold in Rat Subcutaneous Tissue. (A) 2 weeks after implantation; (B) 4 weeks after implantation.

uptake 99% of its dry weight of water including glucose and other molecules. The Epoxy-PU membrane under the scaffold is permeable to glucose and oxygen but impermeable to most interfering substances. GOD immobilized in a BSA/GA matrix is sandwiched between the Pt/Ir wire and the Epoxy-PU membrane. In order to eliminate air bubbles entrapped in the chamber during coating, to stabilize the enzyme gel inside the chamber, and to make the enzyme solution easier to remain in the coil, we used a cotton fiber inside the coil chamber. The collagen scaffolds were prepared by a freeze-drying method and crosslinked to minimize water solubility and enzymatic collagenase degradation. With a light microscope, we confirmed that the porous scaffolds thoroughly surrounded the sensor tips [Fig. 2.8(A) and (B)]. We also observed the surface and cross-sectional morphology of the scaffolds around the sensors using SEM. Many collagen fibrils and uniform open pore structure were observed on the surface [Fig. 2.8(C)]. Inter-connected open pores in the scaffold and a thickness of 150 - 200 μm were observed in cross-sectional region [Fig. 2.8(D)].

The amperometric response curves of the glucose sensors with and without scaffold (control) were obtained by varying the glucose concentration from 5 mM to 15 mM as shown in Figure 2.9. These glucose concentrations were selected because these concentrations were located in the linear response region (2 - 30 mM) of the studied sensors. The results showed no significant response current change before and after scaffold application around the sensor. However, the sensors with scaffolds had a slower response time to reach equilibrium current ($T_{95\%}$) than control sensors. The response time, $T_{95\%}$, is
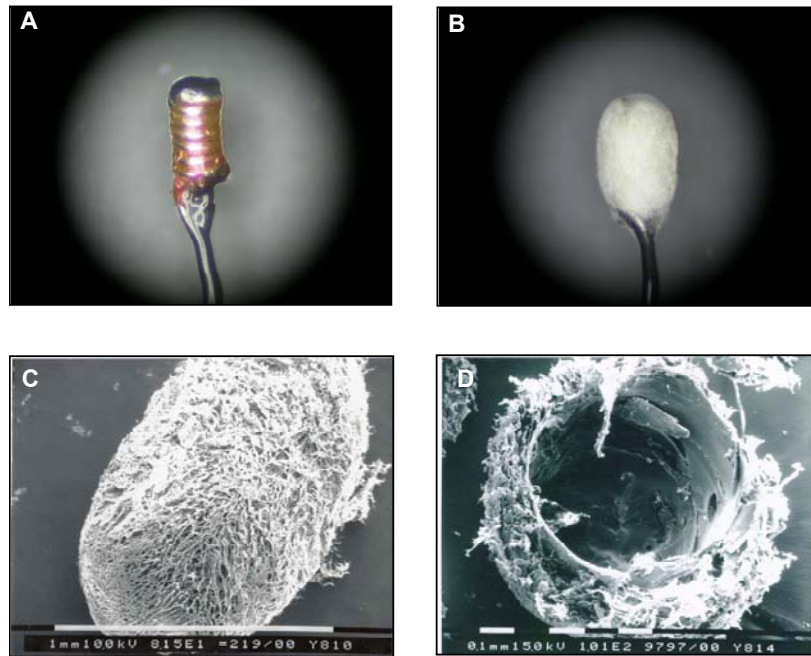
Figure 2.8.   Light Microscope Pictures of the Implantable Glucose Sensing Element and SEM Morphology of the Scaffold Region. (A) Uncoated sensor; (B) Coated with scaffold; (C) Surface; (D) Cross-section.
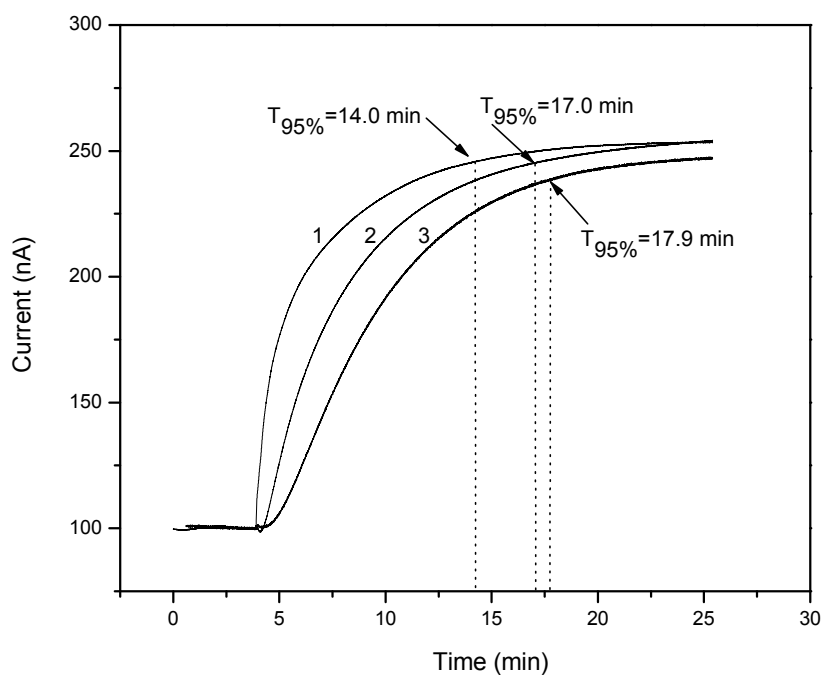
Figure 2.9.   Amperometric Response Curves of the Glucose Sensors from 5 to 15 mM Glucose Concentration. (1) Uncoated sensor; (2) Coated with GA-crosslinked scaffold; (3) Coated with NDGA-crosslinked scaffold. T95% is defined as the time at 95% of the maximum current change ($I_{15\ mM}$ - $I_{5\ mM}$).

44

defined as the time at 95% of the maximum current change ($I_2 - I_1$). The $T_{95\%}$ of control sensor was 14.0 min. whereas $T_{95\%}$ of the sensors with NDGA- and GA-crosslinked scaffold were 17.9 min. and 17.0 min., respectively. The delay of the response time (17.9 and 17 min.) was probably caused by the added physical barrier of the porous scaffolds.

The currents produced by sensors with NDGA-, GA-crosslinked scaffolds and without scaffolds in response to varying glucose concentration (2 - 30 mM) are showed in Figure 2.10. The response currents of the control sensors in the high glucose concentration region (20 - 30 mM) were only a little higher than those of the sensors with scaffolds. However, there was no statistical difference between control and sensors with scaffolds ($p > 0.05$; student t-test). The average sensitivity of the control, NDGA- and GA-crosslinked scaffold around sensors was 11.0, 7.1, and 8.1 nA/mM, respectively. Therefore, scaffold application around the glucose sensors did not negatively affect the function of the sensors.

We also examined the sensitivity changes of the sensors with varying wall thickness of the scaffold controlled by dipping cycles in collagen solution. As can be seen in Figure 2.11, the sensitivity of the 4 times dip-coated sensors remained at 60% of their initial sensitivity (no scaffold). When the sensors were dip-coated more then 5 times, glucose could not diffuse properly through the scaffolds. The sensitivity was dramatically reduced to below 20% of the initial sensitivity. Although the porous scaffold material has good water absorbent properties, the wall thickness can affect the sensor function.

45
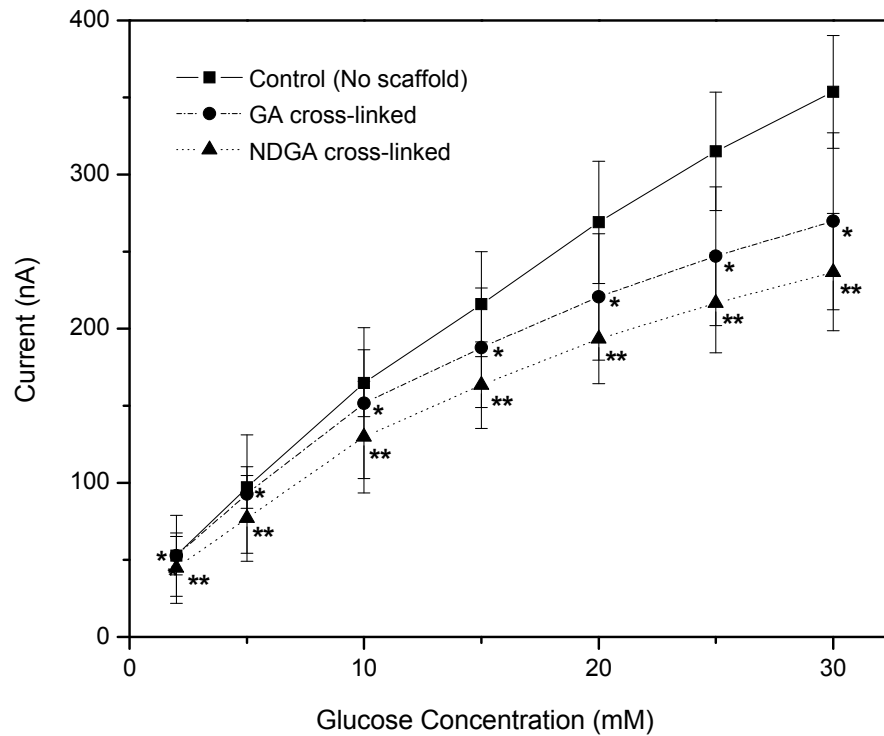
Figure 2.10. Amperometric Response of Uncoated and Collagen Scaffold-coated Glucose Sensors (2-30 mM Glucose). Results are shown as means ± SD (n=3). * Indicates no statistically significant differences between control and GA-crosslinked scaffolds at each glucose concentration (p > 0.05). ** Indicates no statistically significant differences between control and NDGA-crosslinked scaffolds at each glucose concentration (p > 0.05).

46
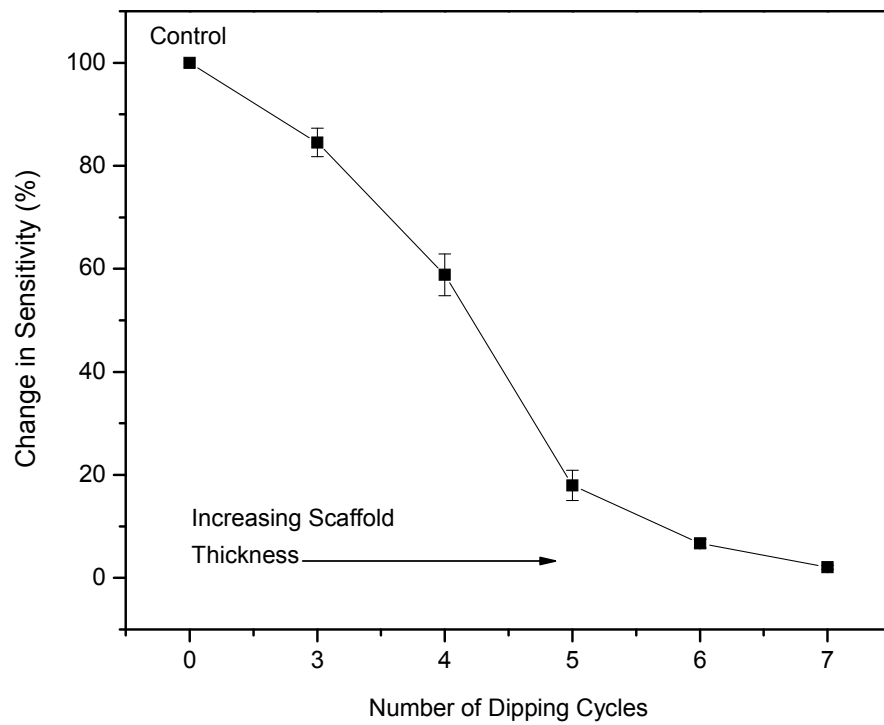
Figure 2.11. Effect of the Scaffold Thickness on Glucose Sensor Sensitivity. Results are shown as means ± SD (n=3).

2.4. Conclusions

In this study, porous type I collagen scaffolds were prepared by a freeze-drying method then crosslinked using NDGA- or GA treatments. The fabricated collagen scaffolds have an open cell and interconnected pore structure. To allow the infiltration neovasculature but to restrict fibrous tissue formation, the mean pore size was controlled to 60 μm by controlling the concentration of the collagen solution. Both crosslinking methods did not significantly affect the scaffolds geometry and bulk properties. They also had a similar resistance property to the collagenase enzyme *in vitro*. However, NDGA-crosslinked scaffolds were shown to be more stable *in vivo*. In addition, we also applied the highly porous NDGA-crosslinked scaffolds to our implantable glucose sensor as a potential approach for reducing "biofouling" and improving biocompatibility. The porous scaffold application did not significantly affect the function of the glucose sensor. Therefore, the application of an NDGA-crosslinked collagen scaffold might be a good candidate for improving the biocompatibility of implantable biosensors. We plan to use this scaffold to enhance the function and lifetime of implantable biosensors by providing a controlled local environment around the sensors with the additional help of various drugs and growth factors.

48

CHAPTER 3

LONG-TERM *IN VITRO* / *IN VIVO* PERFORMANCE OF IMPLANTABLE GLUCOSE SENSORS WITH CROSSLINKED COLLAGEN SCAFFOLDS

3.1. Introduction

Although many strategies for continuous glucose monitoring have been developed over the past 30 years, achieving reliable and continuous glucose monitoring *in vivo* is still a very difficult task. Very often, implantable glucose sensors lose function after a relatively short period of time *in vivo* or become unreliable, despite having excellent *in vitro* performances including good selectivity, a high sensitivity, and a fast response time [33,62,98-100]. This loss of function is in part a consequence of protein adsorption, inflammation, fibrosis encapsulation, and loss of vasculature resulting from the biofouling and the tissue trauma caused by the host response to the sensor and the surgical implantation [20,21,48]. Ultimately, biofouling of the biosensor membrane very much influences glucose diffusion, leading to *in vivo* sensor failures [101,102].

Overall, few successful long term implantations of glucose sensors have been reported. Armour et al. [14] implanted 6 sensors intravascularly in dogs for up to 108 days. Three sensors still functioned with no adherent clots and with the same *in vitro* calibration curves before and after explantation. Updike et al. [103]

49

telemetrically monitored glucose using 3 implanted sensors. The sensor response dropped during the initial period *in vivo* but then rose and stabilized until 42-94 days. The same group (Gilligan et al. [104]) observed a stable foreign body capsule (FBC) around the Dacron or ePTFE velour shells of their implanted sensors. The sensors eventually failed because of enzymatic degradation or biofouling of the sensor membranes. Pickup et al. [26] showed that only 50% of sensors implanted in non-diabetic subjects responded *in vivo*. Explanted sensors examined by scanning electron microscopy were coated by cells and proteins at the sensor tip. Shichiri et al. [38] and Ertefai et al. [13] reported that the *in vivo* lag time was increased, compared to the *in vitro* lag time. The increase was attributed to protein deposition and FBC tissue at the sensor tip.

In order to minimize biofouling and to improve sensor function, many researchers have designed new sensors with modifications to the surface of the sensor outer membrane. Moussy et al. [41,42] introduced a new sensor with a needle-type geometry and a Nafion outermost layer. Quinn et al. [35] used a photo-crosslinkable copolymer containing 2-hydroxyethyl methacrylate (HEMA) and poly(ethylene glycol) (PEG) as a sensor coating material. The results showed that the copolymer-treated electrodes induced much less fibrous tissue than control electrodes due to good biological performance of the PEG material. In order to reproduce lipid characteristics to mimic the cell surface membranes, and induce anti-thrombogenicity, Nishida et al. [105] synthesized a phosphorylcholine (PC)-containing polymer which was applied as a sensor membrane and showed excellent biocompatibility.

50

Because of good swelling and viscoelastic properties and outstanding biocompatibility, many researchers use hydrogels such as PEG hydrogel (Quinn et al. [106]), phenylboronic acid-based hydrogel (Lei et al. [107]), and polyacrylamide hydrogel (Fernandez et al. [108]) as the outermost coating of glucose sensors. Recently, numerous strategies to control delivery of tissue response modifiers (TRM) have been reported. For example, Gifford et al. [109] used nitric oxide (NO) to downregulate mediators of the inflammatory response and Norton et al. [110] characterized VEGF and dexamethasone (Dex) delivery from sensor coatings.

We recently reported the development of new porous collagen scaffolds which were applied around implantable glucose sensors to improve their biocompatibility. We fabricated porous collagen scaffolds by using a freeze-drying method followed by crosslinking using NDGA or GA [111].

In a continuation of this study, we evaluated the sensitivity of sensors with ether NDGA- or GA-crosslinked collagen scaffolds during long-term *in vitro* and *in vivo* experiments. We also fabricated two different lengths of sensors (long and short wires) in order to minimize scaffold damage and compared their function *in vivo* to evaluate the effects of micro-motion on the sensors.

51

3.2. Materials and Methods

3.2.1. Materials

Type I collagen (purified from fetal bovine tendon) was a generous gift from Dr. Thomas Koob, Shriners Hospital for Children (Tampa, FL). Nordihydroguaiaretic acid (NDGA) was purchased from Cayman Chemical Co. (Ann Arbor, MI). Glucose, bovine serum albumin (BSA) and 50% (w/w) glutaraldehyde (GA) were obtained from Fisher Scientific (Pittsburgh, PA). Glucose oxidase (GOD) (EC 1.1.3.4., type X-S, *Aspergillus niger*, 157,500 U/g), epoxy adhesive (ATACS 5104), polyurethane (PU), and tetrahydrofuran (THF) were obtained from Sigma-Aldrich (St. Louis, MO). Dextrose injection solution (50%, w/v) was obtained from Abbott Laboratories (North Chicago, IL). The FreeStyle^{TM} portable glucometer was from TheraSense (Alameda, CA). Sprague-Dawley out-bred rats (male, 375-399 g) were purchased from Harlan (Dublin, VA).

3.2.2. Preparation of Porous Collagen Scaffolds around Implantable Glucose Sensors

We fabricated miniature coil-type glucose sensors loaded with crosslinked enzyme (GOD: glucose oxidase) using a platinum-iridium (Pt/Ir) wire (Teflon coated, Φ 0.125 mm, Pt:Ir = 9:1, Medwire, Sigmund Cohn Corp., Mount Vernon, NY). We applied bovine tendon type I collagen scaffolds around the sensors. Scaffolds were then crosslinked with NDGA or GA treatment as previously described [111] to minimize solubility and to improve resistance to enzymatic degradation *in vivo*. Control sensors (without scaffolds) and sensors

52

with NDGA- or GA-crosslinked scaffolds were equilibrated in phosphate-buffered saline (PBS, 0.1 M NaH_2PO_4, pH 9.0) for 2 days at room temperature prior to being used *in vitro* or *in vivo*.

The initial sensitivity of all sensors was measured in 5 and 15 mM glucose in PBS. Amperometric measurements were performed at room temperature at 0.7 V *vs* Ag/AgCl. The working electrode (Pt/Ir wire) and the Ag/AgCl reference electrode of each sensor were connected to an Apollo 4000 potentiostat (World Precision Instruments, Inc., Sarasota, FL).

In order to investigate the effect of wire length on the sensor function, we fabricated sensors with two different lengths; 10 and 30 mm [Fig 3.1]. Only the wires were of different length, the sensing elements remained identical.

3.2.3. Long-term *In vitro* Characterization of Sensors Coated with Scaffolds

In order to examine the long-term *in vitro* sensitivity of sensors, uncoated (control) sensors, sensors with NDGA-crosslinked collagen scaffolds and sensors with GA-crosslinked collagen scaffolds (n=8 / group) were incubated in PBS at 37°C for 4 weeks. At 7, 14, 21, and 28 days, each sensor was removed and tested in glucose solution.

The sensitivity of the glucose sensors was characterized in glucose/PBS (pH 7.4) at 700 mV versus the incorporated Ag/AgCl reference electrodes. The background current was allowed to stabilize for 10 min., and the sensors were then exposed to a series of glucose solutions in order to examine their sensitivities and linearities.

53
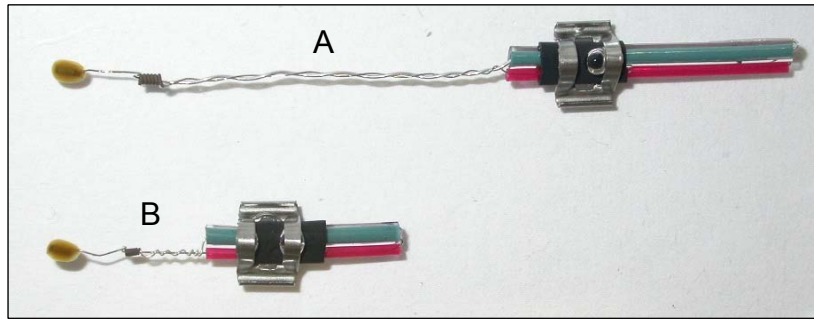
Figure 3.1.   Photograph Showing (A) Long Wire and (B) Short Wire Collagen Scaffold-coated Glucose Sensors.

The response sensitivity (S) was repeatedly assessed by 1) measuring the response current (I_1) of a C_1 glucose solution, 2) adding a concentrated glucose solution into the measured solution to increase the glucose concentration to C_2 and 3) measuring the response current (I_2) of the resulting solution. The sensitivity was expressed as the current increase caused by a 1 mM glucose increase, i.e. $S = (I_2 - I_1) / (C_2 - C_1)$.

3.2.4. Implantation Procedures

All implantable glucose sensors were disinfected using 70% ethanol and then placed in sterile PBS prior to implantation. During the surgical procedure, a continuous flow gas anesthesia system was used to deliver 1.5 % isoflurane to the rats in 2.0 L/min. oxygen flow. All protocols were approved by the University of South Florida Institutional Animal Care and Use Committee (IACUC). Forty-eight sensors (eight control short sensors; CS, eight control long sensors; CL, eight NDGA-crosslinked scaffold around short sensors; NS, eight NDGA-crosslinked scaffold around long sensors; NL, eight GA-crosslinked scaffold around short sensors; GS, and eight GA-crosslinked scaffold around long sensors; GL) were implanted subcutaneously on the back of the rats. Each rat received two of one type of sensors.

For long sensors, two 1.5 cm long longitudinal incisions were made 1.5 cm laterally to the dorsal midline, and 3-4 cm caudally from the neck. A subcutaneous pocket was created using blunt surgical scissors. A 14 ga. I.V. catheter was inserted subcutaneously toward the incision from the 4-5 cm lower

back region. The needle was withdrawn leaving the cannula in the subcutaneous tissue. The sensor wires were carefully fed into the cannula through the incision [Fig. 3.2(A)]. The sensor was secured to the skin by passing a 3-0 Prolene suture through the small gap of the wound clip covering the sensor wires and incisions closed using 3-0 Prolene. The cannula was then withdrawn, leaving the sensor in the subcutaneous tissue.

For short sensors, same-sized incisions were made and a subcutaneous pocket was also created using blunt surgical scissors before implantation. However, the sensors were directly implanted through the incision without using a cannula [Fig. 3.2(B)]. The sensors were secured to the skin and incisions closed using the same approach utilized for the long sensors.

In addition, in order to evaluate the inflammatory response of the tissue around and cellular intrusion into the collagen scaffolds, we directly implanted NDGA- and GA-crosslinked scaffolds (without sensors) in the rats. At set time intervals, tissue samples containing the scaffolds were excised and embedded in paraffin. Sections (5 μm in thickness) were cut and stained with Mayers hematoxylin and eosin (H&E) stain. Stained sections were analyzed and photographed using an Olympus BX41 microscope (Olympus; Tokyo, Japan).

3.2.5. Long-term *In vivo* Evaluation of Sensors Coated with Scaffolds

The sensitivity of each sensor was measured every seven days for up to 28 days or until there was no amperometric response from the implanted sensor. During each measurement period, four rats were anesthetized using isoflurane

56
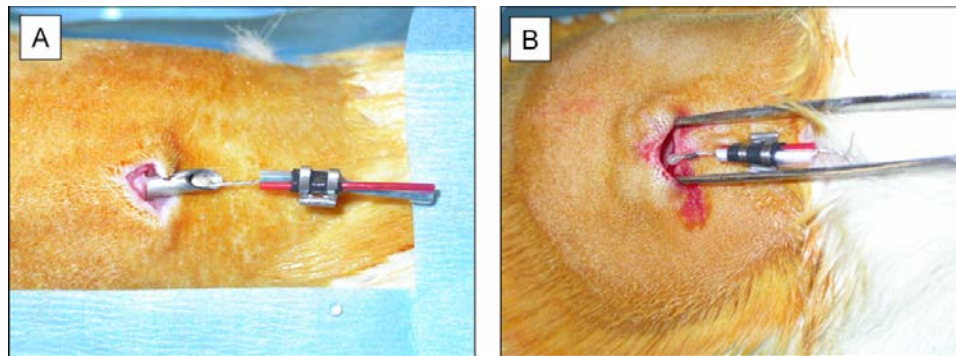
Figure 3.2.   Surgical Procedures by Two Different Implantation Techniques for Long Wire Sensors and Short Wire Sensors. (A) Long wire sensor (using a 14 ga. catheter guidance); (B) Short wire sensors (direct implantation).

and the eight implanted sensors were continuously monitored using two Apollo 4000 potentiostats. After a stable signal was obtained from the sensors, 0.7 mL of sterile 50% dextrose was administered intraperitoneally using a 27 ga. needle. Following the injection, small blood samples were collected every 7 minutes from the rat tail and the glucose level was determined using the standard Freestyle[TM] glucometer. The amperometric response corresponding to the glycemia of the rat was recorded at the corresponding current-time intervals of each sensor. The sensor sensitivity was calculated by dividing the change in current (I) by the change in glycemia (C) between the initial (before dextrose injection) and the peak status (after dextrose injection) as follows: Sensitivity (nA/mM) = $(I_{max} - I_0)$ / $(C_{max} - C_0)$

3.3. Results and Discussion

3.3.1. Preparation of Implantable Glucose Sensors with Porous Crosslinked Collagen Scaffolds

In order to create a porous scaffold for implantable glucose sensors, we first fabricated coil-type glucose sensors loaded with crosslinked enzyme (GOD: glucose oxidase) using platinum-iridium (Pt/Ir) wires. Then, we applied bovine tendon type I collagen scaffolds around the sensors. The collagen scaffolds were prepared by a freeze-drying method and crosslinked using NDGA or GA treatment to minimize their aqueous solubility and reduce their degradation *in vivo*. With a light microscope, we confirmed that the porous scaffolds thoroughly surrounded the working electrodes [Fig. 3.3]. Both scaffolds were semi-transparent in aqueous solution. GA-crosslinked scaffolds appeared white, while the NDGA-crosslinked scaffolds were brown. We also observed high swelling for both scaffolds around the sensors in aqueous solution. We reported previously [111] that these sponge-like matrices with porous inner structure could absorb water above 99%, thus allowing glucose to diffuse freely.

Figure 3.4 shows a schematic of a fully assembled coil-type glucose sensor with a scaffold ready for implantation. The newly assembled sensor is composed of a two-electrode system with a glucose indicating working Pt/Ir electrode and an Ag/AgCl reference-counter electrode. We added a loop between the two electrode coils to avoid micro-shorting caused by the two electrodes touching each other. A surgical wound clip was applied to provide a

59
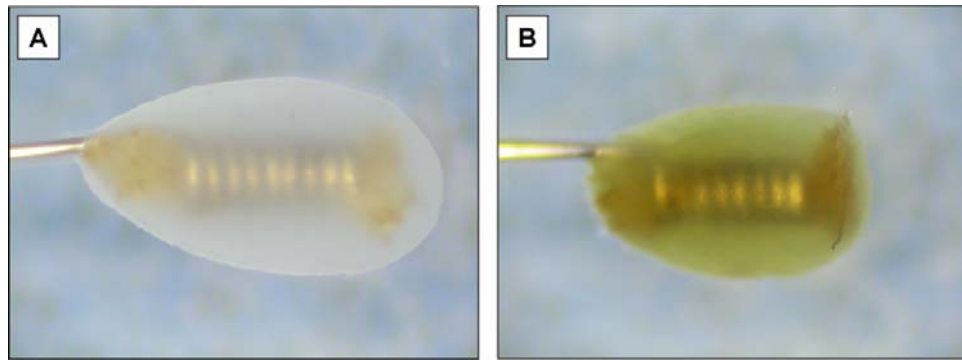
Figure 3.3.   Photographs of Implantable Sensors Coated with (A) GA-crosslinked Porous Collagen Scaffold and (B) NDGA-crosslinked Porous Collagen Scaffold.

60
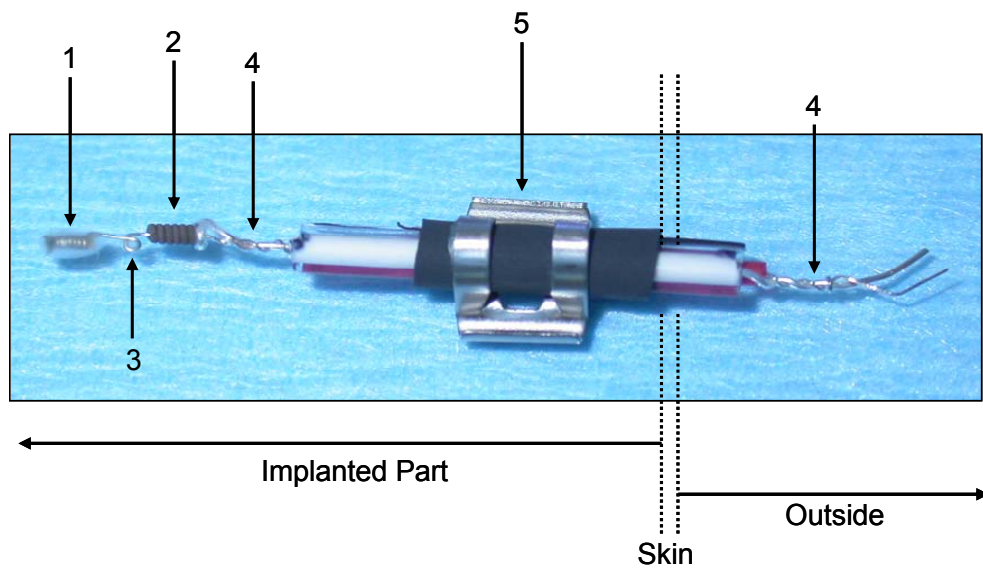
Figure 3.4.   Schematic of Short Wire Implantable Glucose Sensor.
                (1) Pt/Ir working electrode with scaffold;
                (2) Ag/AgCl reference electrode;
                (3) Loop to protect micro-motion and micro-short by two
                     electrodes contact;
                (4) Wires twisted together
                (5) Wound clip

suturing site during the implantation procedure and to prevent the sensor moving out of the skin (i.e. for anchoring).

3.3.2. Long-term *In vitro* Evaluation of Sensors with Porous Collagen Scaffolds

The long-term *in vitro* function of the sensors was determined by tracking their sensitivity for up to 4 weeks. Control sensors (without scaffold), and sensors with NDGA- or GA-crosslinked scaffolds were incubated in PBS at 37°C for up to 4 weeks. The sensors were removed from the PBS at weekly intervals and their sensitivity was determined. The pre-incubation sensitivity (week 0) was measured at the beginning of the *in vitro* study and the percentage of sensitivity change was calculated from the ratio of the sensitivity of the sensors at given time interval to the pre-incubation sensitivity. The sensitivity of all sensors was tested in 5 and 15 mM glucose/PBS. Figure 3.5 shows the sensitivity change of all sensors over 4 weeks. We observed a slight decrease of the sensitivity of sensors with either NDGA- or GA-crosslinked scaffolds, compared to the control (no scaffold) sensors after 1 week incubation. After 2 weeks, the sensitivities of all sensors increased to a level higher than their original sensitivity, probably because of an increase in epoxy-PU membrane permeability due to progressive membrane swelling in aqueous solution. After 2 weeks, the sensitivity of the control sensors, as well as sensors with either NDGA- or GA-crosslinked scaffolds, steadily decreased, however, all sensors retained above 80% of their original sensitivity up to 4 weeks. We believe that the sensitivity decrease after

62
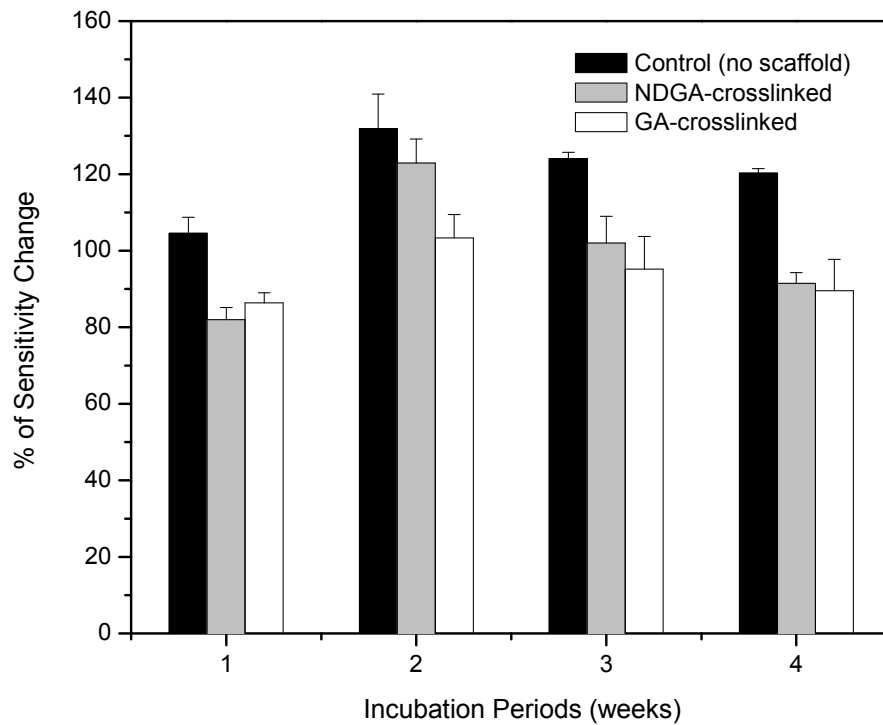
Figure 3.5.   Long-term *In vitro* Sensitivity Changes of Control Sensors and Sensors with NDGA- or GA-crosslinked Collagen Scaffolds. Results are shown as means ± SD.

63

2 weeks may be caused by progressive loss of enzyme activity. Both NDGA and GA-crosslinked scaffolds were still intact around the sensors at week 4. There was no detection of any deformation or detachment of the scaffolds from the sensor membrane surface. Although the overall trend of the sensitivity of the sensors with scaffolds was lower than with the control sensors, the application of scaffolds around sensors did not critically affect the function of the sensors during the 4 week *in vitro* study.

3.3.3. Long-term *In vivo* Performance of Sensors with Porous Collagen Scaffolds

In this study, 48 sensors including control sensors (short/long, CS/CL), and sensors with NDGA- or GA-crosslinked scaffolds (short/long, NS, NL, GS, GL), were implanted subcutaneously in the back of 24 Sprague-Dawley out bred rats for a period of 4 weeks. The *in vivo* sensitivity of every sensor was measured at week 1, 2, 3, and 4. The pre-implantation sensitivity of all sensors was tested using 5 mM and 15 mM glucose/PBS just before implantation. Figure 3.6 shows a photograph of the *in vivo* continuous glucose monitoring procedure with the anesthetized rats. A maximum of 8 sensors were connected to two 4 channels potentiostats. The current produced by the sensors versus time (black arrow) was displayed on two monitors. After reaching a stable signal for 1 – 2 hr, glucose was administered intraperitoneally. Small amounts of blood were sampled every 7 minutes from the rat tail and glucose level was determined using a standard portable glucometer (white arrow).

64
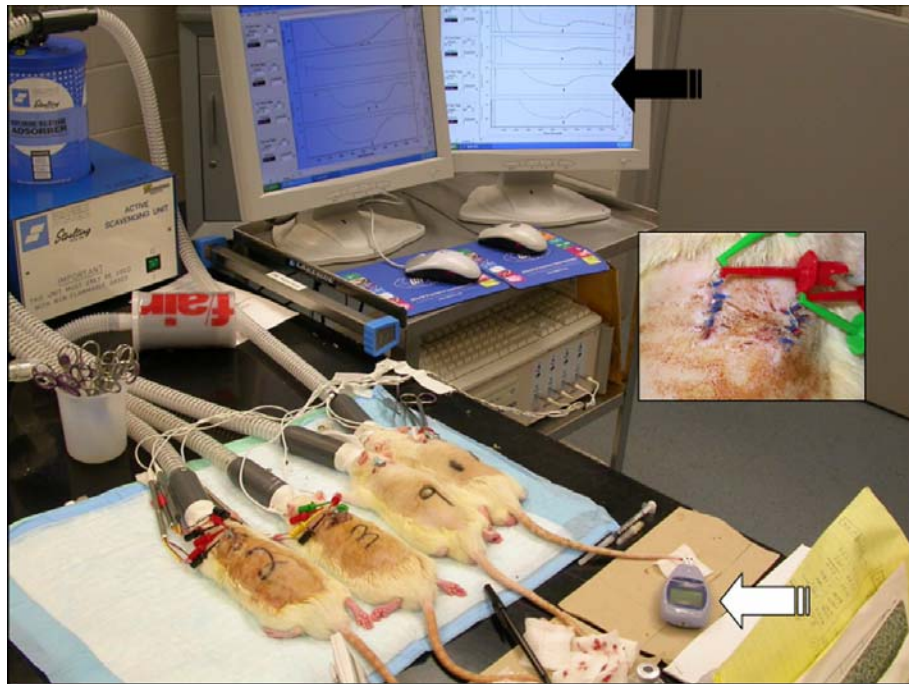
Figure 3.6.   Photograph of *In vivo* Continuous Glucose Monitoring Procedure.

The percentage of sensitivity change for each sensor during the 4 week study is shown in Figure 3.7. From this figure, a few initial observations can be made: 1) The sensitivity of all sensors dramatically decreased after implantation compared to the pre-implantation values. This was probably due to tissue damage which occurred during surgical procedures and the subsequent host response including protein adsorption, blood clot, and the infiltration of inflammatory cells and other cells (e.g. fibroblasts) around the sensor tips [112]. 2) As for the *in vitro* study, the control sensors retained a higher sensitivity than the sensors with scaffolds. The sensors with NDGA-crosslinked collagen scaffolds also had a higher sensitivity than the sensors with GA-crosslinked scaffolds. 3) The sensitivity of the short sensors (CS, NS, GS) appeared to be slightly greater than the sensitivity of the long sensors.

Table 3.1 shows the number of working sensors (used in Figure 3.7) at given time intervals. Initially, 3 sensors did not work at week 1 but regained their function at week 2. Both CS and CL sensors had a higher sensor survival rate (4 out of 8, 6 out of 8, respectively) *in vivo* 4 weeks post implantation than sensors with scaffold coatings. The use of scaffolds worsened the survival rate of the sensors. However, the short sensors had a higher survival rate than the long sensors at 4 weeks post implantation (CL-4, NL-2, GL-1 *vs* CS-6, NS-4, GS-4). We believe that this might result from the long sensors having greater range of motion when the animals move than the short sensors.

66
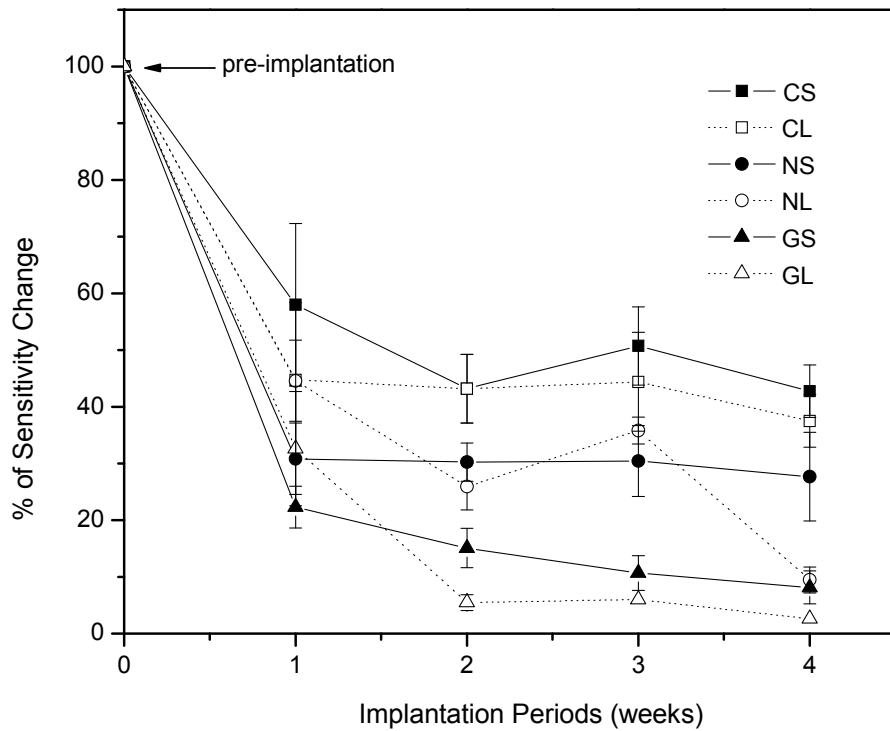
Figure 3.7. Long-term *In vivo* Sensitivity Changes of Control Sensors and Sensors with NDGA- or GA-crosslinked Scaffold. Results are shown as means ± SD. (control short; CS, control long; CL, NDGA-crosslinked scaffold around short sensors; NS, NDGA-crosslinked scaffold around long sensors; NL, GA-crosslinked scaffold around short sensors; GS, GA-crosslinked scaffold around long sensors; GL)

67

Table 3.1. Number of Working Sensors after Implantation. (# out of 8).

Scaffolds	Wire	Weeks after implantation			
		1	2	3	4
Control (no scaffold)	Long	8	7	4	<u>4</u>
	Short	7	8	7	<u>6</u>
NDGA-crosslinked	Long	2	3	2	<u>2</u>
	Short	8	5	5	<u>4</u>
GA-crosslinked	Long	2	2	1	<u>1</u>
	Shot	5	6	6	<u>4</u>

68

The larger macro-/micro-motion may have caused more tissue and scaffold damage. We observed scaffold detached from the working electrode of the long NL sensors [Fig. 3.8(A)], while the NDGA-crosslinked scaffold around the short sensor NS remained in a stable position [Fig. 3.8(B)]. Regarding the GA-crosslinked scaffolds, we could not detect any such scaffold around both long and short sensors [Fig. 3.8(C) and (D)]. This is consistent with our previous study where we observed that the size and shape of the GA-crosslinked scaffolds were dramatically changed (degraded) after 4 weeks of implantation, while the NDGA-crosslinked scaffolds remained mostly intact.

In order to evaluate inflammatory response of the tissue around and within the collagen scaffolds, we directly implanted NDGA- and GA-crosslinked scaffolds (without sensors) in the rats for up to 4 weeks. After 2 weeks implantation, H&E staining revealed the presence of many inflammatory cells including polymorphonuclear (PMN) cells, monocytes, and macrophages within and around the GA-crosslinked scaffolds [Fig. 3.9(A)]. However, for the NDGA-crosslinked scaffolds, few inflammatory cells were observed around the scaffolds, and there was no infiltration of cells in the center region of the scaffolds [Fig. 3.9(B)]. Week 4 showed infiltration of inflammatory cells and fibroblasts, along with granulation tissue deposition inside the pore of the GA-crosslinked scaffolds [Fig. 3.9(C)], and again, less inflammation within and around the NDGA-crosslinked scaffolds [Fig. 3.9(D)]. This result shows that the NDGA-crosslinked collagen scaffolds are more biocompatible than the GA-crosslinked collagen scaffolds and is consistent with a report by Koob et al. [85] showing that NDGA-

69
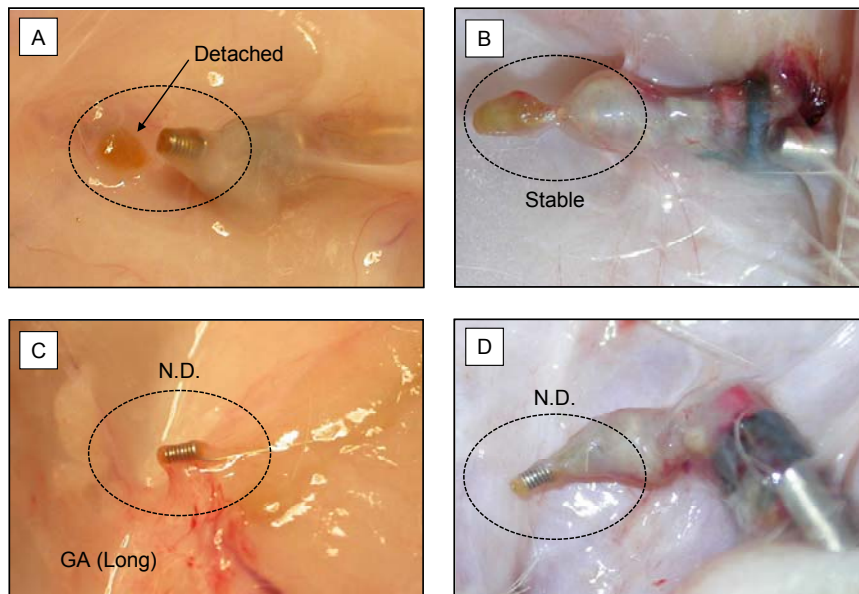
Figure 3.8.   Representative Photograph of Scaffolds *In situ* after 4 Weeks Post Implantation. (A) Long sensor with NDGA-crosslinked scaffold; (B) Short sensor with NDGA-crosslinked scaffold; (C) Long sensor with GA-crosslinked scaffold; (D) Short sensor with GA-crosslinked scaffold.
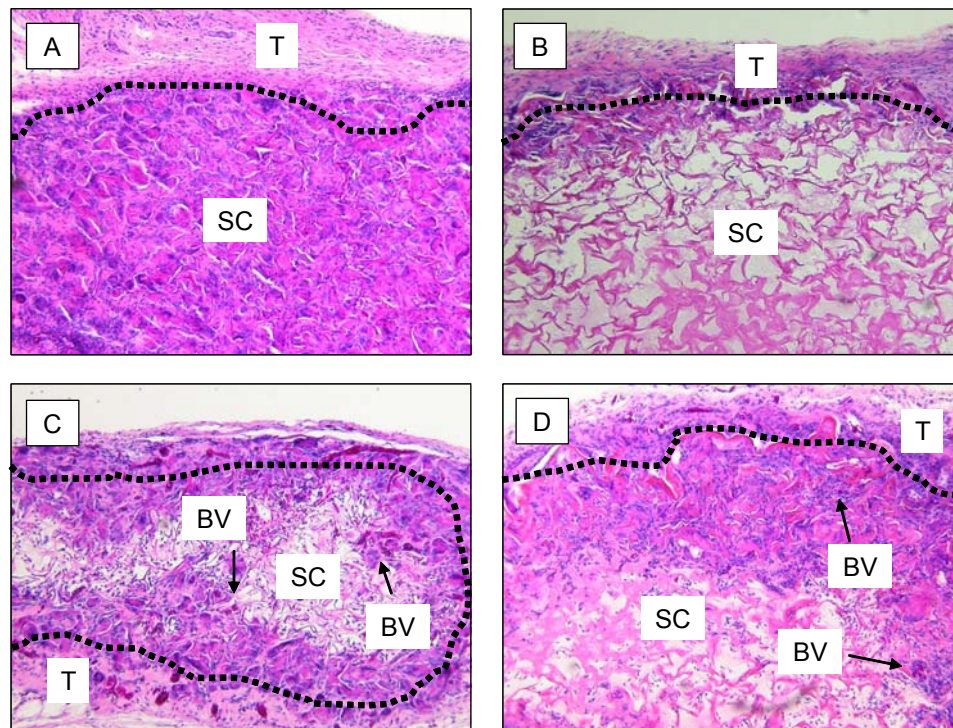
Figure 3.9.   Hematoxylin and Eosin Stained Sections Showing Tissue Surrounding Porous Scaffolds. (A) GA- and (B) NDGA-crosslinked scaffold and after 2 weeks post implantation; (C) GA-and (D) NDGA-crosslinked scaffold after 4 weeks post implantation. (T - tissue surrounding scaffold, SC - scaffold, BV - blood vessels)

crosslinked collagen fibers appeared intact with little foreign body response after implantation in rabbits. The size of the GA-crosslinked scaffolds was reduced and the pore structure was deformed as the implantation time increased. We also found neovasculature in both scaffolds after 4 weeks post-implantation [Fig. 3.9(C) and (D), arrows].

3.4. Conclusions

In this study, we applied porous type I collagen scaffolds around implantable glucose sensors by a freeze-drying method and then crosslinked the scaffolds using NDGA or GA treatments. The fabricated collagen scaffolds had an open cell and interconnected pore structure. All sensors including control sensors (without scaffold), and sensors with NDGA- or GA-crosslinked scaffolds remained functional during the 4 week *in vitro* study. The application of both types of scaffolds around the sensors did not critically affect the function of these sensors *in vitro*.

In the 4 weeks *in vivo* study, the sensitivity of all sensors dramatically decreased (30 – 60%) after 1 week of implantation and then remained relatively stable. The sensitivity and survival rate of the short sensors were higher than the sensitivity of the long sensors possibly as a result of reduced motion within the animals. The sensors with NDGA-crosslinked scaffolds had a higher survival and sensitivity than the sensors with GA-crosslinked scaffolds. By histological examination, we confirmed that the NDGA-crosslinked scaffolds are more biocompatible than the GA-crosslinked scaffolds.

Therefore, this study shows that an NDGA-crosslinked collagen scaffold can be incorporated into the design of our implantable glucose sensor. However, the control sensors (no scaffolds) performed better than the sensors with scaffolds. The scaffolds alone did not improve the function and lifetime of our implantable glucose sensor. This indicates that in order to use these scaffolds as a way to control the local tissue environment around implanted sensors and thus

73

improve their function and lifetime we still need to improve the scaffolds. This could potentially be achieved by using the NDGA-crosslinked collagen scaffold to also deliver various drugs and growth factors to modify the tissue response to the sensors.

CHAPTER 4

DEXAMETHASONE-LOADED PLGA MICROSPHERES/COLLAGEN

SCAFFOLD COMPOSITE SYSTEM FOR IMPLANTABLE

GLUCOSE SENSORS

4.1. Introduction

Although miniaturized implantable glucose sensors show excellent performance *in vitro*, they tend to become unreliable and lose their function after prolonged exposure to the *in vivo* environment, due to the foreign body response (i.e. inflammation, fibrosis, and loss of vasculature) [20,21,48,62,98]. In particular, the accumulation of inflammatory cells and dense fibrotic tissue around the sensor hampers the diffusion of glucose from the capillaries to the sensors [103,113-115]. Despite numerous studies using sensors of several different types, there are no long-term implantable glucose sensors commercially available [62,116].

In order to improve the function of implantable glucose sensors, dexamethasone (Dex, an anti-inflammatory agent) has been used to control the tissue reactions to implanted devices. Dex, a synthetic glucocorticoid, is widely used to suppress inflammatory reactions caused from radiant, mechanical, chemical, infectious and immunological stimuli [50,110,117,118]. It inhibits the

production of critical factors involved in the inflammatory response such as vasoactive/ chemoattractive factors and lipolytic/proteolytic enzymes [50]. Patil et al. [53] prepared Dex-loaded poly(lactic-co-glycolic) acid (PLGA) microspheres/ poly(vinyl alcohol) (PVA) hydrogel composite coatings for implantable biosensors to control detrimental tissue reactions and fibrosis at the sensor/tissue interface. Norton et al. [52,110] reported that they fabricated hydrogel (copolymer; 2-hydroxy-ethyly methacrylate, N-vinyl pyrrolidinon, and polyethylene glycol) sensor coatings containing Dex and/or vascular endothelial growth factor (VEGF) to minimize the foreign body response and to promote angiogenesis. Klueh et al. [62,63] induced significant neovascularization surrounding an implanted sensor using a VEGF-cell-fibrin gene transfer system. Kim and Martin [119] investigated a composite of Dex-loaded PLGA nanoparticles/alginate hydrogel for neural prosthetic application. Lincoff et al. [47] developed a Dex eluting stent using a high molecular weight poly-L-lactic acid (PLLA) biodegradable polymer containing the drug to prevent restenosis. Gomez-Gaete et al. [120] optimized the encapsulation of Dex in PLGA nanoparticles for ocular delivery.

The use of Dex-loaded microspheres/nanospheres to provide controlled local drug delivery are typically prepared using a synthetic biodegradable polymers such as PLGA and PLLA [49]. The degradation rate of these polymers *in vitro*/*in vivo* can be controlled by regulating the composition of monomer units (i.e. lactic acid and glycolic acid). Thus, PLGA microspheres, which have controllable drug release kinetics, have been utilized not only for Dex delivery but also for angiogenic growth factors and other proteins delivery [61,121-123]. Both

76

PLGA and PLLA are also widely used for tissue engineering [124,125] and gene therapy [126] research due to their good biocompatibility and suitable biodegradability characteristics [124-126].

Due to good swelling and viscoelastic properties and outstanding biocompatibility, hydrogels have also been used as sustained-release drug delivery systems and as the outermost coatings of implantable glucose sensors. Pluronics [127-129], also called Poloxamers, are particularly interesting because they are in a sol state below a lower critical solution temperature (LCST; i.e., reverse sol-gel transition temperature, 4-20°C), but transition to a gel state above 37°C [130,131]. Oh et al. [132] fabricated a temperature-controllable crosslinked Pluronic/alginate mixture for use in delivering a non-steroidal anti-inflammatory drug (NSAID) for prevention of post-surgical tissue adhesion.

In this study, we first fabricated porous collagen scaffolds around implantable glucose sensors using a freeze-drying method, followed by crosslinking the collagen scaffold using NDGA treatment [111]. In order to minimize the inflammatory response to the sensors, we then added Dex-loaded microspheres to the scaffold by dipping the sensor/scaffold in a microspheres/Pluronic F127 hydrogel suspension. We characterized the sensors with the Dex-loaded microspheres/ scaffold composite system *in vitro* and then tested these sensors in rats.

77

4.2. Materials and Methods

4.2.1. Materials

Poly(DL-lactide-co-glycolide) (PLGA, Resomer RG503H, 50:50) was a generous gifted from Boehringer-Ingelheim (Germany). Type I collagen (purified from fetal bovine tendon) was a generous gift from Dr. Thomas Koob, Shriners Hospital for Children (Tampa, FL). Nordihydroguaiaretic acid (NDGA) was purchased from Cayman Chemical Co. (Ann Arbor, MI). Methylene chloride (HPLC-GC/MS grade), acetonitrile (HPLC grade), methanol (HPLC grade), glucose, bovine serum albumin (BSA) and 50% (w/w) glutaraldehyde (GA) were obtained from Fisher Scientific (Pittsburgh, PA). Polyvinyl alcohol (PVA; avg. mol. wt = 30,000 - 70,000), dexamethasone (Dex, $C_{22}H_{29}FO_5$; Fw = 392.5), Pluronic F-127, glucose oxidase (GOD) (EC 1.1.3.4., type X-S, *Aspergillus niger*, 157,500 U/g), epoxy adhesive (ATACS 5104), polyurethane (PU), acetone, and tetrahydrofuran (THF) were obtained from Sigma-Aldrich (St. Louis, MO). Dextrose injection solution (50%, w/v) was obtained from Abbott Laboratories (North Chicago, IL). The FreeStyle[TM] glucometer was from TheraSense (Alameda, CA). Sprague-Dawley out-bred rats (male, 375-399 g) were purchased from Harlan (Dublin, VA).

4.2.2. Preparation of Dex-loaded Microspheres

Biodegradable PLGA microspheres loaded with Dex were prepared by an oil-in-water (O/W) emulsion/solvent evaporation technique. The oil phase consisted of 80 mg of PLGA and 50 mg of Dex dissolved in 6 mL of a mixture of

78

either 5:1 methylene chloride to methanol or 5:1 methylene chloride to acetone. This oil phase was added to 100 mL of 0.2% PVA in water, which was stirred with an overhead stirrer at 800 RPM for 30 min. to achieve an O/W emulsion system. The resulting emulsion was stirred on a magnetic stir plate for 16 h to allow complete evaporation of the solvent and solidification of the droplets into microspheres. During the emulsion and solidification process, aluminum foil was completely surrounded the beaker to protect from UV light (UV light will degrade Dex). The microspheres were collected by centrifugation at 8,000 RPM (7,500x g) for 15 min. in a refrigerated centrifuge set at 15°C. The microspheres were washed 5 times with deionized water. The centrifuge tubes were capped and placed in freezer (-20°C) overnight. The tubes were covered with aluminum foil and were placed in a Freeze-drying system overnight to obtain dry microspheres.

4.2.3. Microsphere Analysis

The Dex loading efficiency and encapsulation efficiency into microspheres were determined using high performance liquid chromatography (HPLC) (LC-10AT vp; SPD-10A vp; SCL-10A vp; Shimadzu, Japan). Microspheres (10 mg) were dissolved in 1 mL of acetonitrile. Dex concentration in dissolved samples was determined by HPLC analysis at 246 nm using a Premier C-18 column (Shimadzu, Japan) with a mobile phase of acetonitrile and water mixture (42:58), with flowing mobile phase at 1 mL/min.

79

The drug loading efficiency was calculated using the following equation:

Loading efficiency (%) = mg of Dex / 10 mg of microspheres x 100

The drug encapsulation efficiency was determined using the following equation [133]:

Encapsulation efficiency (%) = experimental drug loading /

theoretical drug loading x 100

The morphology of the microspheres was examined using scanning electron microscopy (SEM) after gold sputter coating of the samples in a metal evaporator according to standard procedures.

4.2.4. Preparation of Dex-loaded Microspheres/Scaffold Composite System

Collagen scaffolds were prepared by a freeze-drying method. Collagen was dissolved in 3% acetic acid to prepare a 1% (w/v) solution. The solution was applied to a cylinder-shaped polypropylene mold (Φ 10 mm, height 8 mm) and then freeze-dried. The scaffolds were then crosslinked with NDGA treatment as follow. Dried collagen scaffolds were briefly soaked in absolute ethanol, followed by soaking in 2 M NaCl in water for 12 h at room temperature. Scaffolds were resuspended in oxygen sparged phosphate buffered saline (PBS, 0.1 M NaH_2PO_4, pH 9.0) for 30 min. at room temperature. Scaffolds were then treated

80

with 3 mg NDGA/mL of PBS prepared as follows: NDGA was dissolved in 0.4 N NaOH at a concentration of 30 mg/mL. One milliliter of the NDGA solution was added directly to 9 mL of PBS containing the scaffold. The scaffolds were agitated in the NDGA solution for 24 h at room temperature. The scaffolds were removed, briefly rinsed with water and freeze-dried.

The microspheres containing Dex were incorporated into the NDGA-crosslinked collagen scaffold by dipping the scaffolds in a microsphere suspensions. Two different microsphere suspension solution (hydrogel and water) were used for fabrication of microsphere/scaffold composites. Pluronic F-127 was adopted as the hydrogel material, using a 25% solution with self-aggregation properties at low critical solution temperature (LCST; i.e., reverse sol-gel transition temperature, 4-20°C) [130-132]. Pluronic solution, freshly prepared by dissolving in deionized water, was kept in the refrigerator (4°C) prior to use. Five, 10, 20 and 40 mg/mL of microspheres, loaded with Dex, were dispersed in the Pluronic solution. Dried scaffolds were soaked in the hydrogel suspension with vortex mixing to incorporate the microspheres evenly. During the procedure, the suspensions were kept in an ice bath to prevent the gelation of Pluronic F-127. After completion of the loading procedure, the microspheres/scaffolds were taken out of the microspheres-hydrogel suspension solution and then placed at room temperature to allow gel formation. Another group of scaffolds were prepared using 5, 10, 20 and 40 mg/mL of microspheres-water suspension at room temperature. In this case, no hydrogel was used. The loading efficiency of Dex in the scaffolds was determined using HPLC as

81

previously described above. Drug concentration was standardized by dividing by total mass of the scaffold including microspheres.

4.2.5. *In vitro* Release of Dex from the Microspheres/Scaffold Composite System

The *in vitro* release study was performed in phosphate buffered saline (PBS) under sink conditions. Samples (1.5 - 2.5 mg) of Dex-loaded microspheres/scaffold composites were incubated in 1 mL of PBS on a heated rocker (Barnstead Lab-Line, US) at a constant temperature (37°C) over 21 days. For comparison, 10 mg of standard Dex-loaded PLGA microspheres were incubated under the same conditions. At 3 or 7 day time intervals, 0.5 mL of supernatant was taken for analysis and replaced with 0.5 mL of fresh PBS into the test tube. Dex concentration of in the samples was determined by HPLC, as described above.

4.2.6. Preparation of Implantable Glucose Sensors with Microspheres/ Scaffold Composite System

We first prepared coil-type glucose sensors loaded with crosslinked enzyme (GOD: glucose oxidase) using a platinum-iridium (Pt/Ir) wire (Teflon coated, Φ 0.125 mm, Pt:Ir = 9:1, Medwire, Sigmund Cohn Corp.). Bovine tendon type I collagen scaffolds were fabricated around the sensors and crosslinked with NDGA as previously described [111].

82

In order to incorporate microspheres loaded with Dex into the scaffolds, the sensors with scaffolds were soaked in either the microsphere-hydrogel suspension or the microsphere-water suspension with vortex mixing as described above. The sensitivities of the sensors (with collagen scaffold only; and with collagen scaffold plus microspheres) were determined in 5 mM and 15 mM glucose/PBS using an Apollo 4000 potentiostat (World Precision Instruments, Inc., Sarasota, FL). Amperometric measurements were performed at room temperature at 0.7 V *vs* Ag/AgCl. The response sensitivity (S) was assessed by 1) measuring the response current (I_1) of a glucose solution (C_1), 2) adding a concentrated glucose solution into the measured solution to increase the glucose concentration (C_2), and 3) measuring the response current (I_2) of the resulting solution. The sensitivity was expressed as the current increase caused by a 1 mM glucose increase, i.e. $S = (I_2 - I_1) / (C_2 - C_1)$.

4.2.7. Implantation Procedures

All implantation protocols were approved by the University of South Florida Institutional Animal Care and Use Committee (IACUC). All implantable glucose sensors were prepared aseptically and then placed in sterile Petri dishes under humidified conditions to prevent the hydrogel from drying. During the surgical procedure, a continuous flow gas anesthesia system was used to deliver 1.5 % isoflurane to the rats in a 2.0 L/min. oxygen flow.

Eight sensors (with microspheres/hydrogel/NDGA-crosslinked collagen scaffold) were implanted subcutaneously on the back of the rats as follows. Two

83

sensors were implanted per rat. Two 1.5 cm long longitudinal incisions were made 1.5 cm laterally to the dorsal midline and 3-4 cm caudally from the neck. A subcutaneous pocket was created using blunt surgical scissors before implantation. The sensors were directly implanted through the incision. The sensors were secured to the skin and the incision was closed using 3-0 Prolene.

In addition, in order to evaluate the inflammatory response to the collagen scaffolds without the influence of the sensor, we directly implanted microspheres/ scaffold samples (without sensors) in the rats. At set time intervals, tissue samples including scaffolds were embedded in paraffin. Sections (ca. 5 μm in thickness) were cut and stained with Mayers hematoxylin and eosin (H&E) stain. Stained sections were analyzed and photographed using an Olympus BX41 microscope (Olympus; Tokyo, Japan).

4.2.8. *In vivo* Evaluation of Sensors Coated with Microspheres/Scaffold Composite System

The sensitivity of implanted sensors was measured every seven days for up to 28 days or until there was no amperometric response from the implanted sensors. During each measurement period, four rats were anesthetized using isofluorane and the eight implanted sensors were continuously monitored using two Apollo 4000 potentiostats. After a stable signal was obtained from the sensors, 0.7 mL of sterile 50% dextrose was administered intraperitoneally using a 27 ga. needle. Following the injection, small blood samples (~ 5 μL) were collected every 7 min. from the rat tail, applied to test strips and the glucose level

84

was determined using the standard Freestyle^{TM} glucometer. The amperometric response corresponding to the glycemia of the rat was recorded at the corresponding current-time intervals of each sensor. The sensor sensitivity was calculated by dividing the change in current (I) by the change in glycemia (C) between the initial (before dextrose injection) and the peak status (after dextrose injection) as follows: Sensitivity (nA/mM) = $(I_{max} - I_0) / (C_{max} - C_0)$

85

4.3. Results and Discussion

4.3.1. Preparation of Dex-loaded PLGA Microspheres

In order to control the release kinetics of Dex, microspheres were fabricated using an oil-water emulsion process. We used PLGA (lactic and glycolic copolymer ratio 50:50) as the biodegradable polymer. The microspheres had a regular spherical morphology as shown in Fig. 4.1. The diameter of Dex-loaded microspheres varied from 1.5 to 50 μm and the average diameter size was 16.0 ± 2.3 μm as estimated from SEM images in three different areas. Figure 4.1(A) shows that many Dex crystals were present around the microspheres because an excess amount of Dex (50 mg in 80 mg of PLGA) was used in the microsphere preparation to increase the Dex loading efficiency. Dex has poor solubility in water, but is freely soluble in alcohols. Washing the microspheres with methanol removed the Dex crystals [Fig. 4.1(B)].

The effect of the organic solvents on Dex encapsulation was investigated using two different organic solvent systems. Methylene chloride (MC) is widely used as an organic solvent for PLGA. Acetone and methanol are good solvents for Dex. A constant ratio of PLGA (80 mg) to Dex (50 mg) and 5 mL of MC were used in this study. Table 4.1 shows Dex loading efficiency and encapsulation efficiency with different solvent systems. The amount of Dex loading and encapsulation efficiency dramatically increased to 14.9 ± 0.51 and 38.9 ± 1.32 %, respectively, when using acetone:MC (1:5), compared to methanol:MC (1:5) (3.3 ± 0.24 and 8.5 ± 0.64 %). Because acetone is also a good solvent for PLGA, the Dex-acetone solution is more miscible with the MC-polymer solution and thus,

86
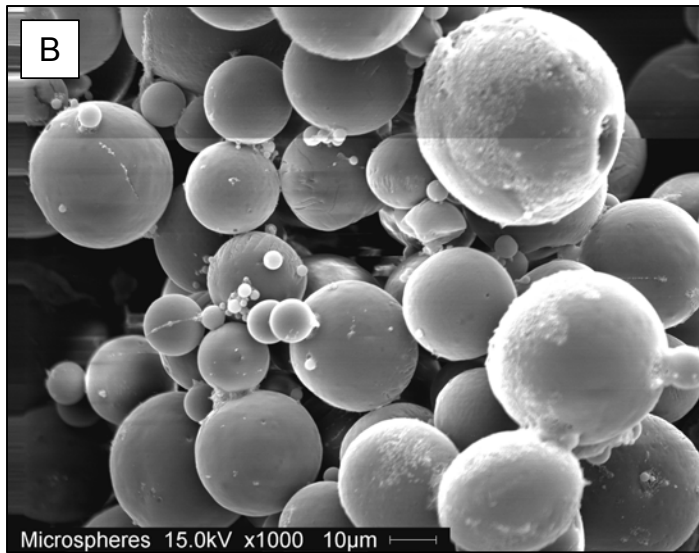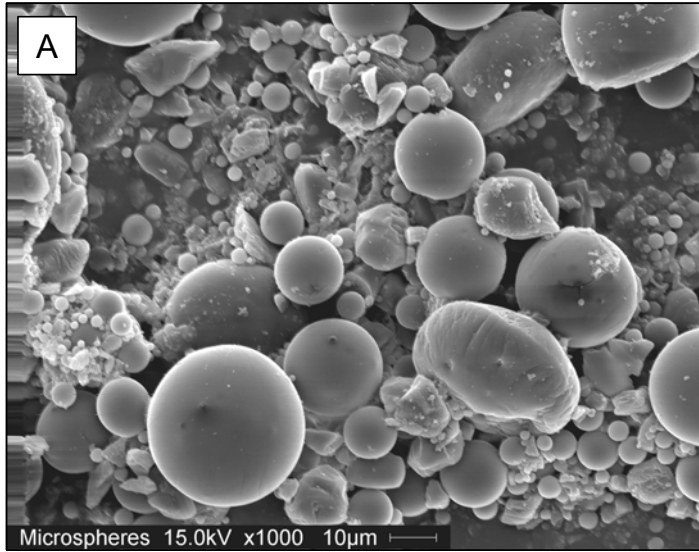
Figure 4.1.   SEM Morphology of the Dex-loaded PLGA Microspheres. (A) with
               Dex crystals; (B) without Dex crystals after washing with methanol.

Table 4.1.   Solvent Effect on the Amount of Dex Loading Efficiency and Encapsulation Efficiency.

Solvent (v:v)	% of Dex Loading (/MS)	Encapsulation Efficiency (%)
Me-OH : MC (1:5)	3.3 ± 0.24	8.5 ± 0.64
Acetone : MC (1:5)	14.9 ± 0.51	38.9 ± 1.32
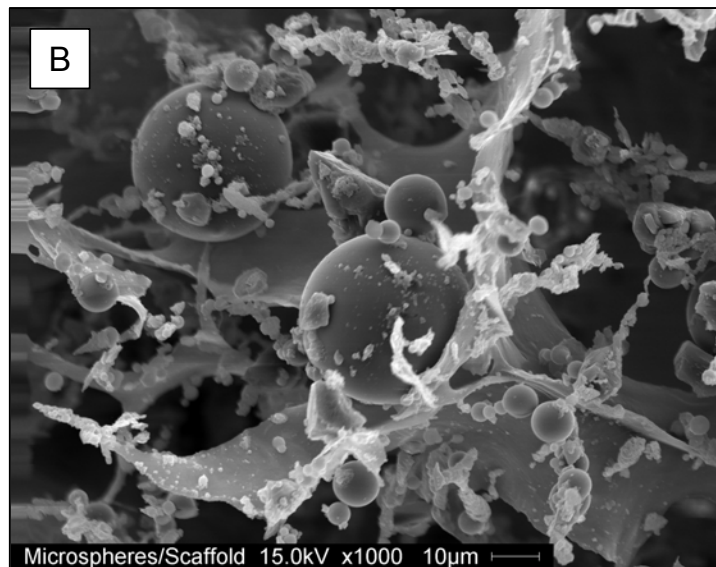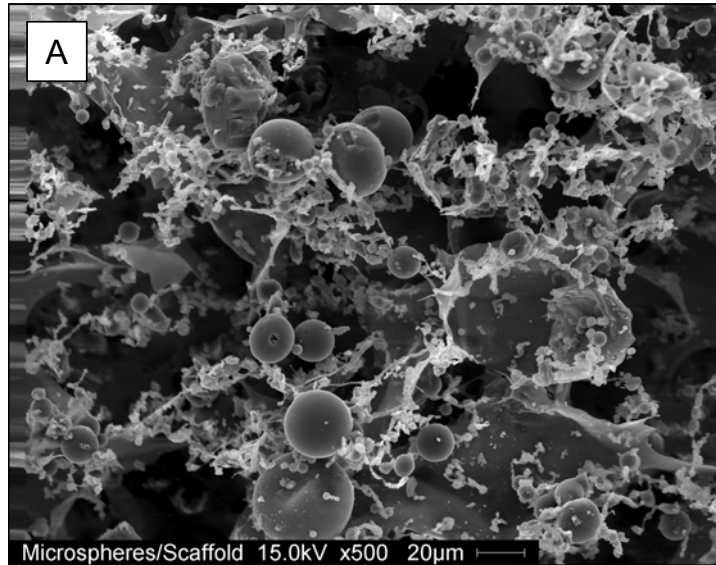
Figure 4.2. SEM Morphology of the Dex-loaded PLGA Microspheres/Collagen Scaffold Composite. (A) x500 magnification; (B) x1,000 magnifications.

the amount of Dex encapsulated in PLGA was higher in the acetone/MC co-solvent system than with the methanol/MC system due to a better continuous phase.

4.3.2. Preparation of Dex-loaded Microspheres/Scaffold Composite System

To further in an effort suppress inflammatory response to implantable glucose sensors, Dex-loaded microspheres were incorporated into the porous NDGA-crosslinked collagen scaffolds. Microspheres suspension in either Pluronic F127 hydrogel or water was used for the fabrication of microspheres/scaffold composites. We chose to add the microspheres to NDGA-crosslinked scaffolds to avoid Dex loss that would have resulted from the crosslinking method in ethanol. Figure 4.2(A) shows that the microspheres were uniformly distributed throughout the scaffold due to its open pores (with diameters ranging from 20 to 100 μm) and high interconnectivity between the pores. In a higher magnification image [Fig. 4.2(B)], the Dex-loaded microspheres (1.5 – 50 μm) can be seen attached to the collagen scaffold matrix.

The effect of different suspensions on drug loading was evaluated. Figure 4.3 shows that the amount of Dex loading efficiency was directly proportional to the initial microsphere-loading amount (5 to 20 mg/mL). Interestingly, the microspheres/scaffold composite fabricated using hydrogel suspension had a much higher loading efficiency than the composite fabricated using water suspension. The Pluronic solution (20% concentration) being highly viscous

90
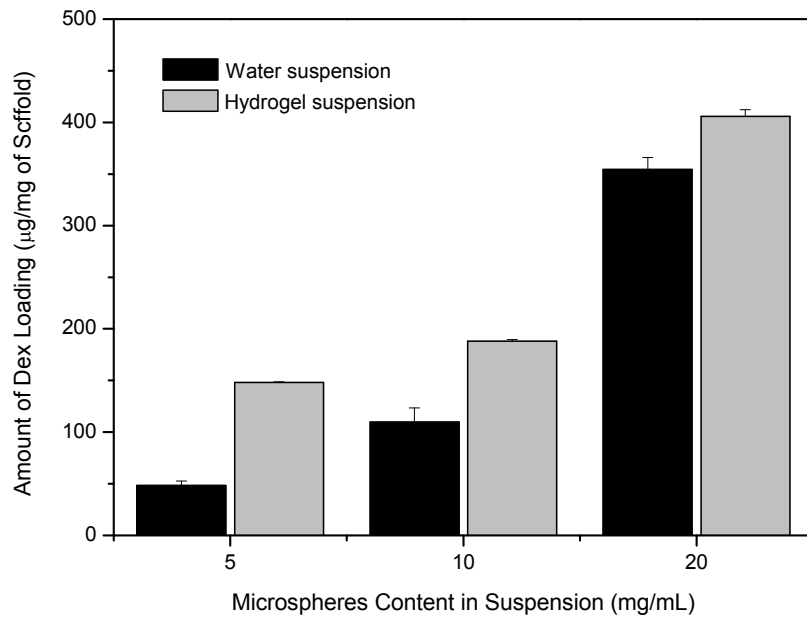
Figure 4.3.   The Amount of Dex Loading in the Composite as Fabricated Using Either Water or Hydrogel Suspension with Different Initial Microspheres Loading Amounts. Results are shown as mean ± SD (n = 4).

91

allowed the addition of many microspheres to the scaffolds during the loading process. In addition, Figure 4.4 shows that the amount of Dex loading decreased from 566.5 ± 1.1 to 510.4 ± 9.0 µg/mg of scaffold after rinsing with water for the microspheres loaded with water suspension. However, there was no significant Dex loss after water rinsing in the composite fabricated using hydrogel suspension. The Pluronic/microspheres mixtures were sol state in the ice bath (below 4°C), but they were gelled at room temperature after the completion of the loading process. We assume that all microspheres still remained in position inside the scaffold after the rinsing step due to this sol-gel transition behavior of the Pluronic suspension.

4.3.3. *In vitro* Drug Release Studies

Four *in vitro* release studies were performed in phosphate buffered saline (PBS) under sink conditions for both microspheres and microspheres/scaffold composite systems. Based on the loading efficiency results above, we chose to fabricate a composite system using the Pluronic hydrogel suspension. At 3 day or 7 day intervals, samples of the incubation medium were collected and Dex concentration in the supernatant was determined by HPLC. Figure 4.5(A) and 4.5(B) show the cumulative Dex release profiles from the PLGA standard microspheres and the PLGA microspheres/collagen scaffold composites, respectively. An initial burst release (20 – 25 %) was observed within 6 – 7 days post incubation for both the microspheres and composite system. The initial burst release was probably due to residual Dex crystals on the surface of the

92
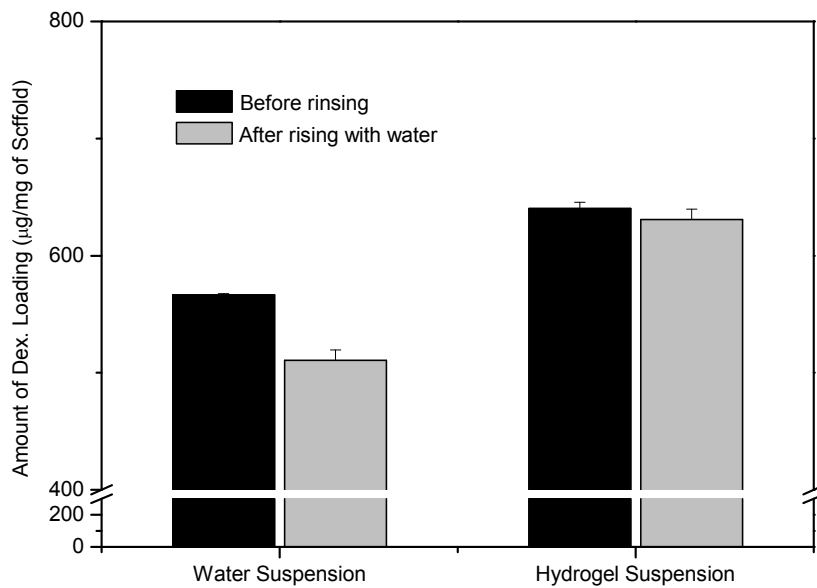
Figure 4.4.   The Amount of Dex Loading in the Composite as Fabricated Using Either Water or Hydrogel Suspension after Rinsing with Water. Results are shown as mean ± SD (n = 4).

93
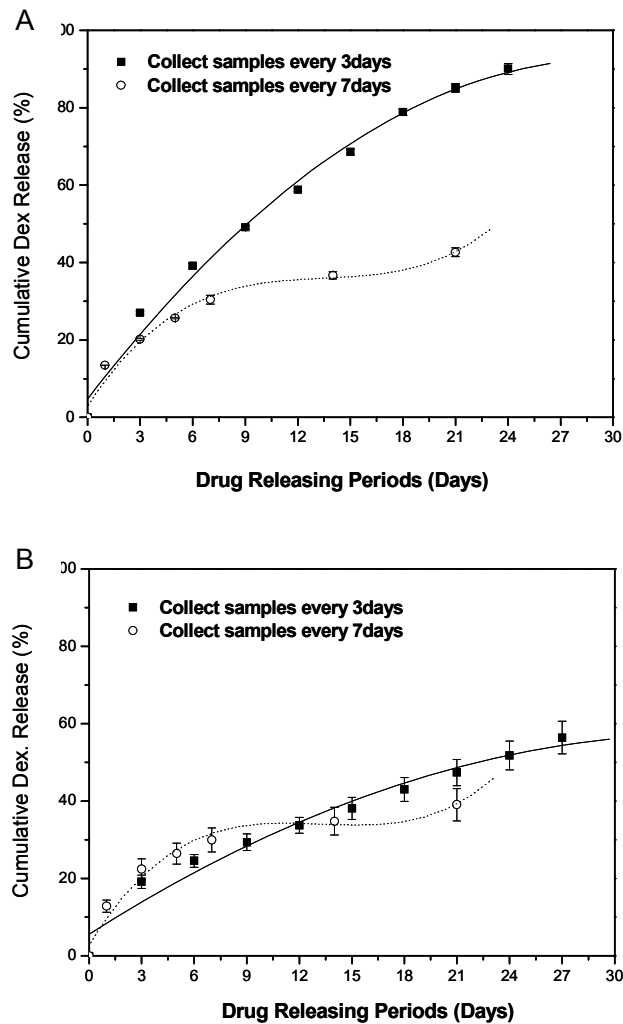
Figure 4.5.   Cumulative Dex Released from Standard Microspheres and Dex-loaded Microspheres/Scaffold Composite During the *In vitro* Release Studies in PBS at 37°C. The total amount of Dex released into the PBS as a percentage of the total amount of Dex encapsulated into the microspheres (A) and encapsulated into the scaffold composites (B) was plotted as a function of the elapsed time from the beginning of the release studies. Results are shown as means ± SD (n = 4).

94

microspheres [50,53]. For the three day interval sample collection shows that the release of Dex from microspheres alone reached 90% release within 24 days, while the composite system released 50% of Dex during the same period. The composite system dramatically slowed the drug release compared to the standard microspheres. This result may suggest that either collagen scaffold or the hydrogel phase in the scaffold delayed Dex diffusion to the releasing media.

The release profile of both microspheres and composite system when collected at 7 day intervals showed the same pattern with an initial burst release and continued zero order release pattern between day 7 and day 21, probably because of inadequate sink condition (PBS was replaced every 7 days). Nonetheless, the release study with 3 day sample collection showed sustained release of Dex from the microsphere/hydrogel/scaffold system over 1 month.

4.3.4. Implantable Glucose Sensors Covered with Microspheres/Scaffold Composite System

We prepared coil-type glucose sensors with porous collagen scaffolds as previously described [111]. Then, Dex-loaded microspheres were incorporated into the scaffolds surrounding the sensors by soaking in microspheres-Pluronic suspensions. With a light microscope, we confirmed that the microspheres thoroughly surrounded the sensor surface [Fig. 4.6(A)]. In a higher magnification image [Fig. 4.6(B)], the Dex-loaded microspheres were observed to be uniformly distributed inside the pore structure of the collagen scaffold.

95
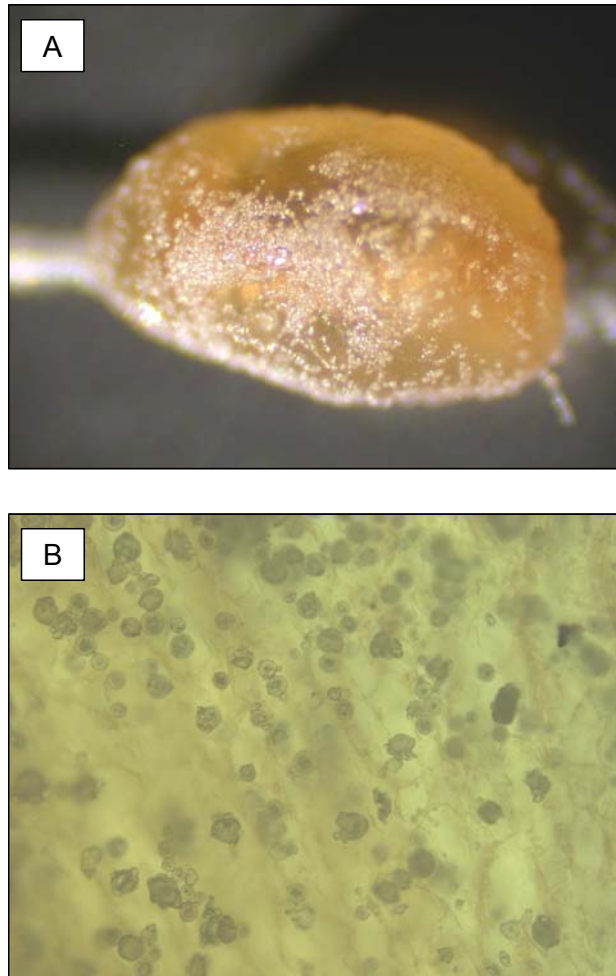
Figure 4.6.   Light Microscope Photographs of the Implantable Glucose Sensing Element with Dex-loaded Microspheres/Scaffold Composite. (A) Working electrode; (B) x100 magnification of the scaffold region.

The effect of the microspheres on the function of sensors was investigated by varying the glucose concentration from 5 to 15 mM. The sensitivity change for each sensor before and after microspheres application with different suspensions is shown in Figure 4.7. We observed a slight decrease of the sensitivity of sensors with microspheres fabricated using either water or hydrogel suspension, compared to the sensors without microspheres. However, there was no statistical difference before and after microspheres application ($p > 0.05$; Student's t-test). Therefore, adding microspheres around the sensors with scaffold did not negatively intact the function of the sensors.

4.3.5. *In vivo* Performance of Sensors with Dex-loaded Microspheres/ Scaffold Composite System

Implantable glucose sensors with Dex-loaded microspheres/scaffold composite were implanted subcutaneously in the back of rats and their sensitivity measured for up to 28 days or until there was no amperometric response. Because of higher Dex loading, we chose to fabricate the composite system using the Pluronic hydrogel suspension containing 40 mg/mL of Dex-loaded microspheres. Figure 4.8 shows the percent sensitivity change of the sensors during the 2 week study. The sensitivity of the sensors with composite was compared to our previous *in vivo* data results (without microspheres; control, NDGA-crosslinked scaffold, GA-crosslinked scaffold). The sensors with the composite system retained above 50% of their original sensitivity at 2 weeks,

97
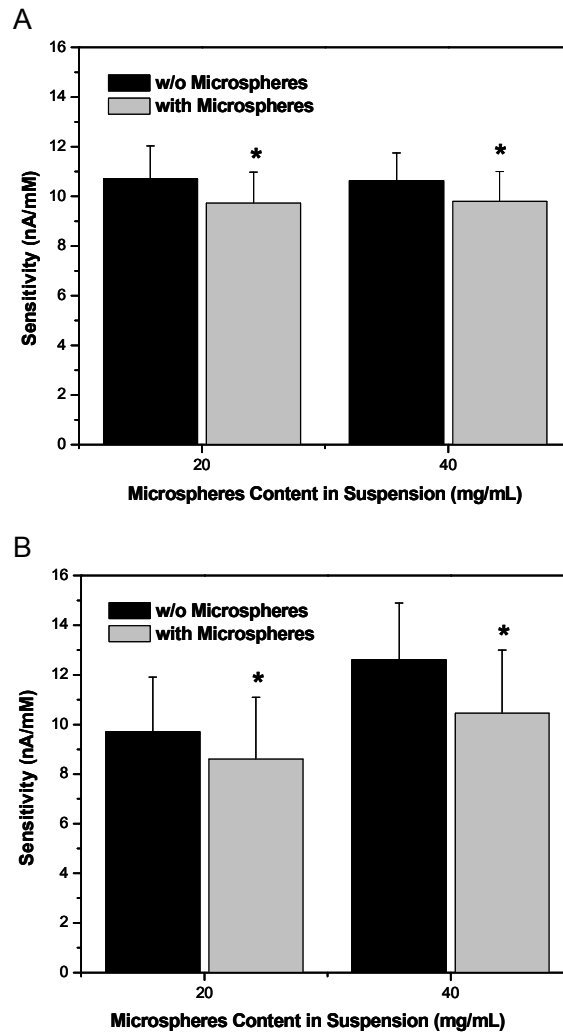
Figure 4.7.   Effect of Adding PLGA Microspheres in the Scaffold on Glucose Sensor Sensitivity with Different Suspensions. (A) Water suspension; (B) Pluronic F127 hydrogel suspension. Results are shown as means ± SD. (n = 4). *Indicates no statistically significant differences before / after incorporation of microspheres (p > 0.05).

98
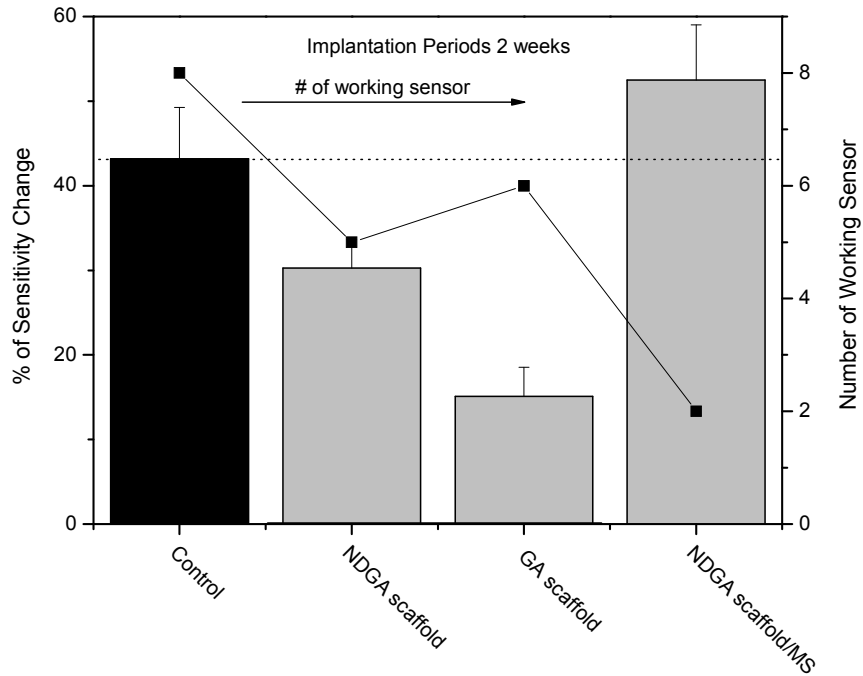
Figure 4.8. *In vivo* Sensitivity Changes (Bar Graph - results are shown as means ± SD) and Number of Working Sensors (Line Graph) of Control Sensors and Sensors with NDGA- or GA-crosslinked Collagen Scaffolds and Sensors with Dex-loaded Microspheres/ NDGA-crosslinked Collagen Scaffold after 2 Weeks Post Implantation.

99

while the sensitivity of the control sensors, sensors with NDGA-crosslinked scaffolds and sensors with GA-crosslinked scaffolds decreased to 42%, 30%, and 15%, respectively. We believe that this was because the locally delivered Dex effectively decreased the inflammatory response to the sensors. However, it was observed that only 2 out of 8 sensors with the composite scaffolds functioned at 2 weeks. We suggest that the reason for the functional failure may be related to the reference electrode [Fig. 4.9(A)]. Figure 4.9(B) shows a dense fibrous capsule surrounding the reference electrode. In this study, we applied Dex-loaded microspheres/scaffold composite around the working electrode but not around the reference electrode. For this study, we did not coil the reference electrode to avoid micro-shorting caused by touching reference electrode coil (Ag/AgCl wire) to the uncovered Pt/Ir wire. However, this different reference electrode geometry may have induced a larger inflamed area of tissue.

After 4 weeks, we excised non-functional sensors and tested them *ex vivo* (with tissue) in 5 mM and 15 mM glucose/PBS. Subsequently, the sensors were removed from the surrounding tissue and tested *in vitro*. Figure 4.10 shows the amperometric response curves of an explanted glucose sensor with and without fibrous capsule tissue. It was found that the sensor with its fibrous capsule responded poorly (line A, sensitivity = 1.5 nA/mM) to changes in glucose concentration, while the sensor regained its initial function (line B, sensitivity = 15.4 nA/mM) after removing the surrounding tissue. These shows that the dense fibrous capsule tissue which forms around the reference electrode can also affect

100
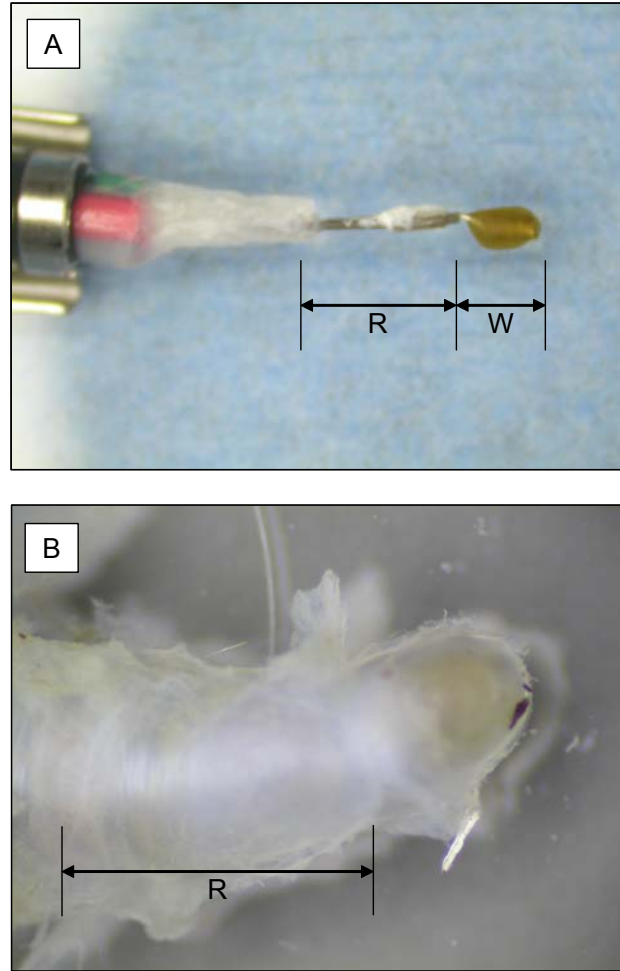
Figure 4.9.   Light Microscope Photographs of Implantable Glucose Sensors. (A) Reference and working electrode region; (B) Dense fibrous capsule tissue surrounding the reference electrode (R - reference electrode, W - working electrode).
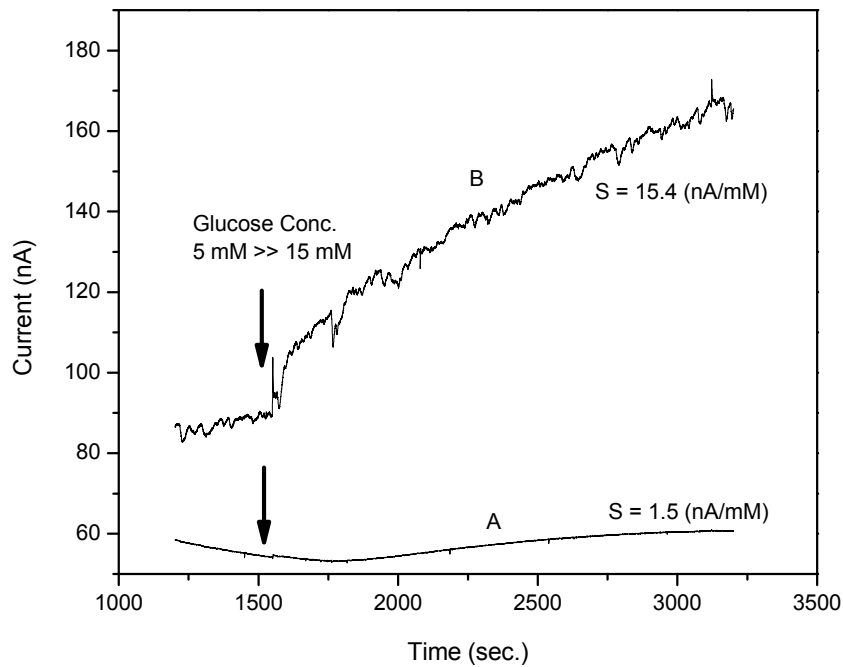
Figure 4.10. Amperometric Response Curves of the Explanted Non-functioned Glucose Sensors after 4 Weeks Post Implantation. (A) *Ex vivo* response of the sensor with surrounding fibrous capsule tissue; (B) *In vitro* response of the sensor after removing surrounding the fibrous capsule tissue, after glucose concentration increase from 5 to 15 mM.

102

the sensor. Thus, the reference electrode could also be surrounded by the composite system described in this paper.

4.3.6. Suppression of Inflammation to Dex-loaded Microspheres/Scaffold Composite System

To confirm the anti-inflammatory response of the Dex-loaded microspheres/scaffold composite (40 mg/mL of microspheres, Pluronic F127 hydrogel suspension), we implanted the composites (without sensors) subcutaneously in rats. Standard NDGA-crosslinked scaffolds (without microspheres) were implanted for comparison. The histological results (H&E stain) for sampled at 2 and 4 weeks after implantation for both the scaffold alone and the composite scaffold are shown in Figure 4.11. The inflammatory cells were stained as purple, while normal cells were stained as pink. A very strong inflammatory response was shown around the control scaffold 2 weeks after implantation [Fig. 4.11(A)]. Predominant polymorphonuclear leukocytes (PMNs) with monocytes and macrophages were observed and a dense connective tissue layer (fibrous capsule) surrounded the periphery of the scaffold. In contrast, the inflammatory response to the Dex-loaded composites [Fig. 4.11(B)] was diminished compared to the control scaffold. The histological results after one week implantation are not shown as there was no noticeable difference between the control scaffold and the Dex-loaded composites. After 4 weeks post implantation, the inflammatory response to the Dex-released composites was low [Fig. 4.11(D)] while a severe inflammatory response with a thick fibrous capsule

103
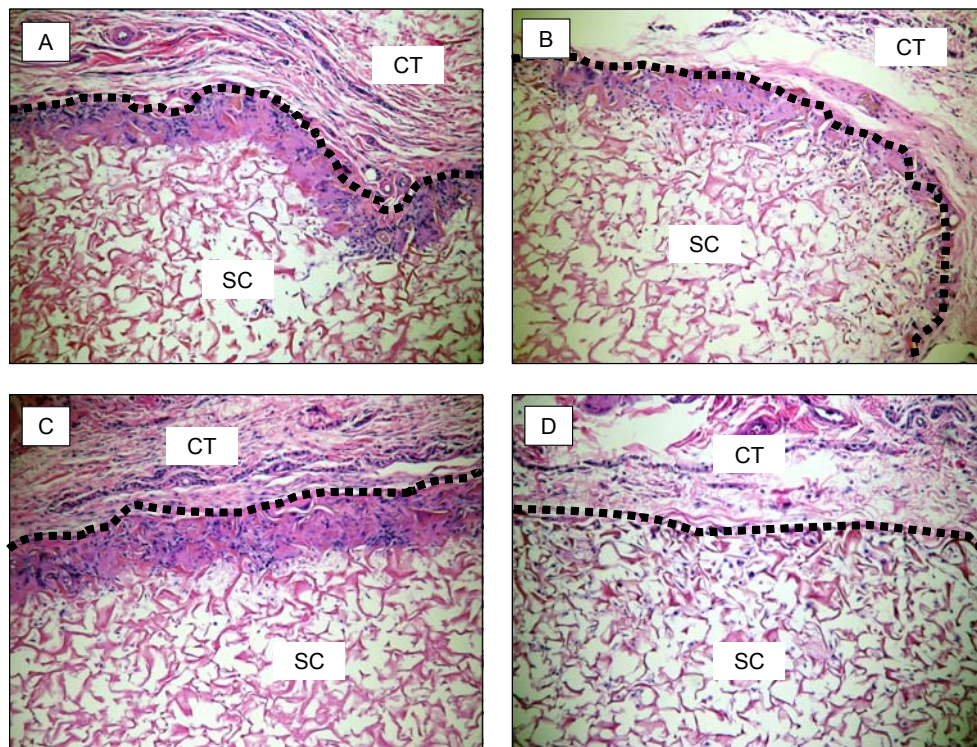
Figure 4.11. Hematoxylin and Eosin Stained Sections of Tissue Surrounding Porous Scaffolds in Rats. (A) NDGA-crosslinked scaffold; (B) Dex-loaded microspheres / NDGA-crosslinked scaffold composite after 2 weeks post implantation; (C) NDGA-crosslinked scaffold; (D) Dex-loaded microspheres / NDGA-crosslinked scaffold composite after 4 weeks post implantation (CT - connective tissue, SC-scaffold).

104

was present around the scaffold without Dex-loaded microspheres [Fig. 4.11(C)]. These results demonstrate that the Dex released from the microspheres/scaffold greately reduced the inflammatory response to the scaffold.

4.4. Conclusions

In this study, we prepared Dex-loaded PLGA microspheres and incorporated then into three dimensional porous type I collagen scaffolds (crosslinked with NDGA) around implantable glucose sensors. The fabricated composite has effectively loaded Dex and sustained release of Dex for at least one month. The composite system did not significantly alter the function of the sensors *in vitro* despite the high amount of microspheres. After 2 weeks *in vivo*, the sensitivity of sensors with the composite system remained higher than for other sensors without the composite system. The histological results showed that the inflammatory response was lowered using the Dex-loaded composite scaffold when compared to the inflammatory response to the scaffolds without Dex-loaded microspheres at 2 and 4 weeks after implantation. These results showed that our Dex-loaded composite system reduces inflammation around the implanted glucose sensors tips and could potentially improve their function and lifetime.

CHAPTER 5

SUGGESTIONS FOR FUTURE STUDY

The best tissue environment for implantable biosensor is vascularized tissue around sensor. The control of neovascularization has recently focused on the use of angiogenic growth factors such as VEGF and PDGF. Norton et al. [52,110] reported that they fabricated hydrogel sensor coatings containing Dex and/or VEGF to minimize foreign body response and to promote angiogenesis. Klueh et al. [62,63] induced significant neovascularization surrounding an implanted sensor using a VEGF-cell-fibrin gene transfer system.

The goal future studies will be to introduce local delivery with microsphere systems to release angiogenic factors (VEGF, PDGF) and anti-inflammatory drugs (i.e. dexmethasone), concurrently. Since Dex can lead to an anti-angiogenesis effect along with an anti-inflammatory response, the optimization of the concentrations of either angiogenic factors or Dex will play an important role in the dual release system. The future investigations should determine how to control neovasculrature density without foreign body response around implanted glucose sensors. In addition, we found a dense fibrous capsule surrounding the reference electrode in Chapter 4. In future investigations, the reference electrode should also be coated with the same approach utilized for the working electrode.

107

REFERENCES

1.   ADA. American Diabetes Association - All about diabetes. URL - http://www.diabetes.org/about-diabetes.jsp 2008.

2.   Newman JD, Turner AP. Home blood glucose biosensors: a commercial perspective. Biosens Bioelectron 2005;20(12):2435-53.

3.   Heller A. Implanted electrochemical glucose sensors for the management of diabetes. Annu Rev Biomed Eng 1999;1:153-75.

4.   NIH-NIDDK. National Institute of Diabetes and Digestiv and Kidney Diseases - Diabetes overview. URL - http://diabetes.niddk.nih.gov/dm/pubs/overview/DiabetesOverview.pdf 2008.

5.   ADA. American Diabetes Association; Self-monitoring of blood glucose. Diabetes Care 1994;17(1):81-6.

6.   Lee S, Nayak V, Dodds J, Pishko M, Smith NB. Glucose measurements with sensors and ultrasound. Ultrasound Med Biol 2005;31(7):971-7.

7.   Moussy F, Harrison DJ, O'Brien DW, Rajotte RV. Performance of subcutaneously implanted needle-type glucose sensors employing a novel trilayer coating. Anal Chem 1993;65(15):2072-7.

8.   Johnson KW, Mastrototaro JJ, Howey DC, Brunelle RL, Burden-Brady PL, Bryan NA, Andrew CC, Rowe HM, Allen DJ, Noffke BW and others. In vivo evaluation of an electroenzymatic glucose sensor implanted in subcutaneous tissue. Biosens Bioelectron 1992;7(10):709-14.

9.   Koudelka M, Rohner-Jeanrenaud F, Terrettaz J, Bobbioni-Harsch E, de Rooij NF, Jeanrenaud B. In-vivo behaviour of hypodermically implanted microfabricated glucose sensors. Biosens Bioelectron 1991;6(1):31-6.

10.   Bindra DS, Zhang Y, Wilson GS, Sternberg R, Thevenot DR, Moatti D, Reach G. Design and in vitro studies of a needle-type glucose sensor for subcutaneous monitoring. Anal Chem 1991;63(17):1692-6.

11.   Pickup JC, Shaw GW, Claremont DJ. In vivo molecular sensing in diabetes mellitus: an implantable glucose sensor with direct electron transfer. Diabetologia 1989;32(3):213-7.

12.   Shichiri M, Asakawa N, Yamasaki Y, Kawamori R, Abe H. Telemetry glucose monitoring device with needle-type glucose sensor: a useful tool for blood glucose monitoring in diabetic individuals. Diabetes Care. Volume 9; 1986. p 298-301.

13.   Ertefai S, Gough DA. Physiological preparation for studying the response of subcutaneously implanted glucose and oxygen sensors. J Biomed Eng 1989;11(5):362-8.

14.   Armour JC, Lucisano JY, McKean BD, Gough DA. Application of chronic intravascular blood glucose sensor in dogs. Diabetes 1990;39(12):1519-26.

15.   Frost MC, Meyerhoff ME. Implantable chemical sensors for real-time clinical monitoring: progress and challenges. Curr Opin Chem Biol 2002;6(5):633-41.

16.   Ash SR, Poulos JT, Rainier JB, Zopp WE, Janle E, Kissinger PT. Subcutaneous capillary filtrate collector for measurement of blood glucose. Asaio J 1992;38(3):M416-20.

17.   Meyerhoff C, Bischof F, Sternberg F, Zier H, Pfeiffer EF. On line continuous monitoring of subcutaneous tissue glucose in men by combining portable glucosensor with microdialysis. Diabetologia 1992;35(11):1087-92.

18.   Moscone D, Mascini M. Microdialysis and glucose biosensor for in vivo monitoring. Ann Biol Clin (Paris) 1992;50(5):323-7.

19.   Joseph JI, Torjman MJ. Glucose Sensors. In: Wnek GE, Bowlin GL, editors. Encyclopedia of biomaterials and biomedical engineering. New York: Marcel Dekker; 2004. p 683-692.

20.	Reichert WM, Saavedra SS. Materials considerations in the selection, performance, and adhesion of polymeric encapsulants for implantable sensors. In: Williams DF, editor. Medical and Dental Materials. New York: VCH Publishers, Inc.; 1992. p 303-343.

21.	Reichert WM, Sharkawy AA. Chap. 28 Biosonsors In: Von Recum A, editor. Handbook of biomaterials evaluation : scientific, technical, and clinical testing of implant materials. Philadelphia: Taylor & Francis; 1999. p 439-460.

22.	Sharkawy AA, Neuman MR, Reichert WM. Sensocompatibility: Design considerations for biosensor-based drug delivery systems. In: Park K, editor. Controlled Drug Delivery: The Next Generation. Washington, DC: American Chemical Society; in Press.

23.	Clark LC, Jr., Lyons C. Electrode systems for continuous monitoring in cardiovascular surgery. Ann N Y Acad Sci 1962;102:29-45.

24.	Updike SJ, Hicks GP. The enzyme electrode. Nature 1967;214(92):986-8.

25.	Gough DA, Leypoldt JK, Armour JC. Progress toward a potentially implantable, enzyme-based glucose sensor. Diabetes Care 1982;5(3):190-8.

26.	Pickup JC, Claremont DJ, Shaw GW. Responses and calibration of amperometric glucose sensors implanted in the subcutaneous tissue of man. Acta Diabetol 1993;30(3):143-8.

27.	Abel PU, von Woedtke T. Biosensors for in vivo glucose measurement: can we cross the experimental stage. Biosens Bioelectron 2002;17(11-12):1059-70.

28.	Anderson JM. Chapter 4 Mechanisms of inflammation and infection with implanted devices. 1993;2(3, Supplement 1):33.

29.	Johnston RB, Jr. Current concepts: immunology. Monocytes and macrophages. N Engl J Med 1988;318(12):747-52.

30.	Maciag T. Molecular and cellular mechanisms of angiogenesis. Important Adv Oncol 1990:85-98.

31.   Thompson JA, Anderson KD, DiPietro JM, Zwiebel JA, Zametta M, Anderson WF, Maciag T. Site-directed neovessel formation in vivo. Science 1988;241(4871):1349-52.

32.   Ziats NP, Miller KM, Anderson JM. In vitro and in vivo interactions of cells with biomaterials. Biomaterials 1988;9(1):5-13.

33.   Sharkawy AA, Klitzman B, Truskey GA, Reichert WM. Engineering the tissue which encapsulates subcutaneous implants. I. Diffusion properties. J Biomed Mater Res 1997;37(3):401-12.

34.   Cannas M, Bosetti M, Santin M, Mazzarelli S. 2. Tissue response to implants: Molecular interactions and histological correlation. In: Wise DL, editor. Biomaterials and bioengineering handbook. New York: Marcel Dekker; 2000. p 95-117.

35.   Quinn CP, Pathak CP, Heller A, Hubbell JA. Photo-crosslinked copolymers of 2-hydroxyethyl methacrylate, poly(ethylene glycol) tetra-acrylate and ethylene dimethacrylate for improving biocompatibility of biosensors. Biomaterials 1995;16(5):389-96.

36.   Rigby GP, Crump P, Vadgama P. Open flow microperfusion: approach to in vivo glucose monitoring. Med Biol Eng Comput 1995;33(2):231-4.

37.   Reddy SM, Vadgama PM. Ion exchanger modified PVC membranes--selectivity studies and response amplification of oxalate and lactate enzyme electrodes. Biosens Bioelectron 1997;12(9-10):1003-12.

38.   Shichiri M, Yamasaki Y, Nao K, Sekiya M, Ueda N. In vivo characteristics of needle-type glucose sensor--measurements of subcutaneous glucose concentrations in human volunteers. Horm Metab Res Suppl 1988;20:17-20.

39.   Shaw GW, Claremont DJ, Pickup JC. In vitro testing of a simply constructed, highly stable glucose sensor suitable for implantation in diabetic patients. Biosens Bioelectron 1991;6(5):401-6.

40.   Wilkins E, Atanasov P, Muggenburg BA. Integrated implantable device for long-term glucose monitoring. Biosens Bioelectron 1995;10(5):485-94.

111

41.   Moussy F, Jakeway S, Harrison DJ, Rajotte RV. In vitro and in vivo performance and lifetime of perfluorinated ionomer-coated glucose sensors after high-temperature curing. Anal Chem 1994;66(22):3882-8.

42.   Moussy F, Harrison DJ, Rajotte RV. A miniaturized Nafion-based glucose sensor: in vitro and in vivo evaluation in dogs. Int J Artif Organs 1994;17(2):88-94.

43.   Moussy F, Harrison DJ. Prevention of the rapid degradation of subcutaneously implanted Ag/AgCl reference electrodes using polymer coatings. Anal Chem 1994;66(5):674-9.

44.   Kerner W, Kiwit M, Linke B, Keck FS, Zier H, Pfeiffer EF. The function of a hydrogen peroxide-detecting electroenzymatic glucose electrode is markedly impaired in human sub-cutaneous tissue and plasma. Biosens Bioelectron 1993;8(9-10):473-82.

45.   Reil TD, Sarkar R, Kashyap VS, Sarkar M, Gelabert HA. Dexamethasone suppresses vascular smooth muscle cell proliferation. J Surg Res 1999;85(1):109-14.

46.   Kawamura M, Hatanaka K, Saito M, Ogino M, Ono T, Ogino K, Matsuo S, Harada Y. Are the anti-inflammatory effects of dexamethasone responsible for inhibition of the induction of enzymes involved in prostanoid formation in rat carrageenin-induced pleurisy? Eur J Pharmacol 2000;400(1):127-35.

47.   Lincoff AM, Furst JG, Ellis SG, Tuch RJ, Topol EJ. Sustained local delivery of dexamethasone by a novel intravascular eluting stent to prevent restenosis in the porcine coronary injury model. J Am Coll Cardiol 1997;29(4):808-16.

48.   Wisniewski N, Moussy F, Reichert WM. Characterization of implantable biosensor membrane biofouling. Fresenius J Anal Chem 2000;366(6-7):611-21.

49.   Burgess DJ, Hickey AJ. Microsphere Technology and Applications In: Swarbrick J, Boylan JC, editors. Encyclopedia of Pharmaceutical Technology: Marcel Dekker Inc; 1994. p 1-29.

50.	Hickey T, Kreutzer D, Burgess DJ, Moussy F. Dexamethasone/PLGA microspheres for continuous delivery of an anti-inflammatory drug for implantable medical devices. Biomaterials 2002;23(7):1649-56.

51.	Hickey T, Kreutzer D, Burgess DJ, Moussy F. In vivo evaluation of a dexamethasone/PLGA microsphere system designed to suppress the inflammatory tissue response to implantable medical devices. J Biomed Mater Res 2002;61(2):180-7.

52.	Norton LW, Tegnell E, Toporek SS, Reichert WM. In vitro characterization of vascular endothelial growth factor and dexamethasone releasing hydrogels for implantable probe coatings. Biomaterials 2005;26(16):3285-97.

53.	Patil SD, Papadimitrakopoulos F, Burgess DJ. Dexamethasone-loaded poly(lactic-co-glycolic) acid microspheres/poly(vinyl alcohol) hydrogel composite coatings for inflammation control. Diabetes Technol Ther 2004;6(6):887-97.

54.	Yancopoulos GD, Davis S, Gale NW, Rudge JS, Wiegand SJ, Holash J. Vascular-specific growth factors and blood vessel formation. Nature 2000;407(6801):242-8.

55.	Darland DC, D'Amore PA. Blood vessel maturation: vascular development comes of age. J Clin Invest 1999;103(2):157-8.

56.	Lokmic Z, Idrizi R, Messina A, Knight KR, Morrison W, Mitchell G. Vascularization of Engineered Constructs. In: Wnek GE, Bowlin GL, editors. Encyclopedia of biomaterials and biomedical engineering. New York: Marcel Dekker; 2004. p 1750-1759.

57.	Benjamin LE, Hemo I, Keshet E. A plasticity window for blood vessel remodelling is defined by pericyte coverage of the preformed endothelial network and is regulated by PDGF-B and VEGF. Development 1998;125(9):1591-8.

58.	Ennett AB, Mooney DJ. Tissue engineering strategies for in vivo neovascularisation. Expert Opin Biol Ther 2002;2(8):805-18.

59.   Prokop A, Kozlov E, Nun Non S, Dikov MM, Sephel GC, Whitsitt JS, Davidson JM. Towards retrievable vascularized bioartificial pancreas: induction and long-lasting stability of polymeric mesh implant vascularized with the help of acidic and basic fibroblast growth factors and hydrogel coating. Diabetes Technol Ther 2001;3(2):245-61.

60.   Chen RR, Mooney DJ. Polymeric growth factor delivery strategies for tissue engineering. Pharm Res 2003;20(8):1103-12.

61.   Richardson TP, Peters MC, Ennett AB, Mooney DJ. Polymeric system for dual growth factor delivery. Nat Biotechnol 2001;19(11):1029-34.

62.   Klueh U, Dorsky DI, Kreutzer DL. Use of vascular endothelial cell growth factor gene transfer to enhance implantable sensor function in vivo. J Biomed Mater Res A 2003;67(4):1072-86.

63.   Klueh U, Dorsky DI, Kreutzer DL. Enhancement of implantable glucose sensor function in vivo using gene transfer-induced neovascularization. Biomaterials 2005;26(10):1155-63.

64.   Ward WK, Quinn MJ, Wood MD, Tiekotter KL, Pidikiti S, Gallagher JA. Vascularizing the tissue surrounding a model biosensor: how localized is the effect of a subcutaneous infusion of vascular endothelial growth factor (VEGF)? Biosens Bioelectron 2003;19(3):155-63.

65.   Sheu MT, Huang JC, Yeh GC, Ho HO. Characterization of collagen gel solutions and collagen matrices for cell culture. Biomaterials 2001;22(13):1713-9.

66.   Pieper JS, van der Kraan PM, Hafmans T, Kamp J, Buma P, van Susante JL, van den Berg WB, Veerkamp JH, van Kuppevelt TH. Crosslinked type II collagen matrices: preparation, characterization, and potential for cartilage engineering. Biomaterials 2002;23(15):3183-92.

67.   Chvapil M, Kronenthal L, Van Winkle W, Jr. Medical and surgical applications of collagen. Int Rev Connect Tissue Res 1973;6:1-61.

68.   Pachence JM. Collagen-based devices for soft tissue repair. J Biomed Mater Res 1996;33(1):35-40.

69.   Lee CH, Singla A, Lee Y. Biomedical applications of collagen. Int J Pharm 2001;221(1-2):1-22.

70.   Ramshaw JA, Werkmeister JA, Glattauer V. Collagen-based biomaterials. Biotechnol Genet Eng Rev 1996;13:335-82.

71.   Ramshaw JAM, Glattauer V, Werkmeister JA. Stabilization of collagen in medical devices. In: Wise DL, editor. Biomaterials and bioengineering handbook. New York: Marcel Dekker; 2000. p 717-738.

72.   Sano A, Hojo T, Maeda M, Fujioka K. Protein release from collagen matrices. Adv Drug Deliv Rev 1998;31(3):247-266.

73.   Friess W. Collagen--biomaterial for drug delivery. Eur J Pharm Biopharm 1998;45(2):113-36.

74.   Griffith M, Hakim M, Shimmura S, Watsky MA, Li F, Carlsson D, Doillon CJ, Nakamura M, Suuronen E, Shinozaki N and others. Artificial human corneas: scaffolds for transplantation and host regeneration. Cornea 2002;21(7 Suppl):S54-61.

75.   Barbani N, Giusti P, Lazzeri L, Polacco G, Pizzirani G. Bioartificial materials based on collagen: 1. Collagen cross-linking with gaseous glutaraldehyde. J Biomater Sci Polym Ed 1995;7(6):461-9.

76.   Nimni ME, Cheung B, Strates B, Kodama M, Sheikh K. Bioprosthesis derived from crosslinked and chemically modified collageneous tissue. In: Nimni ME, editor. Collagen Vol. III - Biotechnology. Boca Raton, FL: CRC Press; 1998. p 1-38.

77.   Huang-Lee LL, Cheung DT, Nimni ME. Biochemical changes and cytotoxicity associated with the degradation of polymeric glutaraldehyde derived crosslinks. J Biomed Mater Res 1990;24(9):1185-201.

78.   van Luyn MJ, van Wachem PB, Olde Damink LH, Dijkstra PJ, Feijen J, Nieuwenhuis P. Secondary cytotoxicity of cross-linked dermal sheep collagens during repeated exposure to human fibroblasts. Biomaterials 1992;13(14):1017-24.

115

79.   Khor E. Methods for the treatment of collagenous tissues for bioprostheses. Biomaterials 1997;18(2):95-105.

80.   Sung HW, Hsu HL, Shih CC, Lin DS. Cross-linking characteristics of biological tissues fixed with monofunctional or multifunctional epoxy compounds. Biomaterials 1996;17(14):1405-10.

81.   Chvapil M. Considerations on manufacturing principles of a synthetic burn dressing: a review. J Biomed Mater Res 1982;16(3):245-63.

82.   Chvapil M, Speer D, Mora W, Eskelson C. Effect of tanning agent on tissue reaction to tissue implanted collagen sponge. J Surg Res 1983;35(5):402-9.

83.   Lee CR, Grodzinsky AJ, Spector M. The effects of cross-linking of collagen-glycosaminoglycan scaffolds on compressive stiffness, chondrocyte-mediated contraction, proliferation and biosynthesis. Biomaterials 2001;22(23):3145-54.

84.   Tsai CL, Hsu Sh SH, Cheng WL. Effect of different solvents and crosslinkers on cytocompatibility of Type II collagen scaffolds for chondrocyte seeding. Artif Organs 2002;26(1):18-26.

85.   Koob TJ. Biomimetic approaches to tendon repair. Comp Biochem Physiol A Mol Integr Physiol 2002;133(4):1171-92.

86.   Koob TJ, Hernandez DJ. Material properties of polymerized NDGA-collagen composite fibers: development of biologically based tendon constructs. Biomaterials 2002;23(1):203-12.

87.   Koob TJ, Willis TA, Hernandez DJ. Biocompatibility of NDGA-polymerized collagen fibers. I. Evaluation of cytotoxicity with tendon fibroblasts in vitro. J Biomed Mater Res 2001;56(1):31-9.

88.   Koob TJ, Willis TA, Qiu YS, Hernandez DJ. Biocompatibility of NDGA-polymerized collagen fibers. II. Attachment, proliferation, and migration of tendon fibroblasts in vitro. J Biomed Mater Res 2001;56(1):40-8.

89.   Harkness RD. Collagen. Sci Prog 1966;54(214):257-74.

90.   Stenzel KH, Dunn MW, Rubin AL, Miyata T. Collagen gels: design for a vitreous replace- ment. Science 1969;164(885):1282-3.

91.   Miyata T, Sode T, Rubin AL, Stenzel KH. Effects of ultraviolet irradiation on native and telopeptide-poor collagen. Biochim Biophys Acta 1971;229(3):672-80.

92.   Gorham SD, Light ND, Diamond AM, Willins MJ, Bailey AJ, Wess TJ, Leslie NJ. Effect of chemical modifications on the susceptibility of collagen to proteolysis. II. Dehydrothermal crosslinking. Int J Biol Macromol 1992;14(3):129-38.

93.   Long N, Yu B, Moussy Y, Moussy F. Strategies for testing long-term transcutaneous amperometric glucose sensors. Diabetes Technol Ther 2005;7(6):927-36.

94.   Yu B, Long N, Moussy Y, Moussy F. A long-term flexible minimally-invasive implantable glucose biosensor based on an epoxy-enhanced polyurethane membrane. Biosens Bioelectron 2006;21(12):2275-82.

95.   Koob TJ. Collagen Fixation. In: Wnek GE, Bowlin GL, editors. Encyclopedia of biomaterials and biomedical engineering. New York: Marcel Dekker; 2004. p 335-347.

96.   Patel VR, Amiji MM. Preparation and characterization of freeze-dried chitosan-poly(ethylene oxide) hydrogels for site-specific antibiotic delivery in the stomach. Pharm Res 1996;13(4):588-93.

97.   Angele P, Abke J, Kujat R, Faltermeier H, Schumann D, Nerlich M, Kinner B, Englert C, Ruszczak Z, Mehrl R and others. Influence of different collagen species on physico-chemical properties of crosslinked collagen matrices. Biomaterials 2004;25(14):2831-41.

98.   Mercado RC, Moussy F. In vitro and in vivo mineralization of Nafion membrane used for implantable glucose sensors. Biosens Bioelectron 1998;13(2):133-45.

99.   Sharkawy AA, Klitzman B, Truskey GA, Reichert WM. Engineering the tissue which encapsulates subcutaneous implants. II. Plasma-tissue exchange properties. J Biomed Mater Res 1998;40(4):586-97.

100.   Sharkawy AA, Klitzman B, Truskey GA, Reichert WM. Engineering the tissue which encapsulates subcutaneous implants. III. Effective tissue response times. J Biomed Mater Res 1998;40(4):598-605.

101.   Pfeiffer EF. On the way to the automated (blood) glucose regulation in diabetes: the dark past, the grey present and the rosy future. XII Congress of the International Diabetes Federation, Madrid, 22-28 September 1985. Diabetologia 1987;30(2):51-65.

102.   Clark LC, Jr., Noyes LK, Spokane RB, Sudan R, Miller ML. Long-term implantation of voltammetric oxidase/peroxide glucose sensors in the rat peritoneum. Methods Enzymol 1988;137:68-89.

103.   Updike SJ, Shults MC, Rhodes RK, Gilligan BJ, Luebow JO, von Heimburg D. Enzymatic glucose sensors. Improved long-term performance in vitro and in vivo. Asaio J 1994;40(2):157-63.

104.   Gilligan BJ, Shults MC, Rhodes RK, Updike SJ. Evaluation of a subcutaneous glucose sensor out to 3 months in a dog model. Diabetes Care 1994;17(8):882-7.

105.   Nishida K, Sakakida M, Ichinose K, Uemura T, Uehara M, Kajiwara K, Miyata T, Shichiri M, Ishihara K, Nakabayashi N. Development of a ferrocene-mediated needle-type glucose sensor covered with newly designed biocompatible membrane, 2-methacryloyloxyethyl phosphorylcholine-co-n-butyl methacrylate. Med Prog Technol 1995;21(2):91-103.

106.   Quinn CA, Connor RE, Heller A. Biocompatible, glucose-permeable hydrogel for in situ coating of implantable biosensors. Biomaterials 1997;18(24):1665-70.

107.   Lei M, Baldi A, Nuxoll E, Siegel RA, Ziaie B. A hydrogel-based implantable micromachined transponder for wireless glucose measurement. Diabetes Technol Ther 2006;8(1):112-22.

118

108.   Fernandez E, Lopez-Cabarcos E, Mijangos C. Viscoelastic and swelling properties of glucoe oxidase loaded polyacrylamide hydrogels and the evaluation of their properties as glucose sensors. Polymer 2005;46(7):2211-2217.

109.   Gifford R, Batchelor MM, Lee Y, Gokulrangan G, Meyerhoff ME, Wilson GS. Mediation of in vivo glucose sensor inflammatory response via nitric oxide release. J Biomed Mater Res A 2005;75(4):755-66.

110.   Norton LW, Koschwanez HE, Wisniewski NA, Klitzman B, Reichert WM. Vascular endothelial growth factor and dexamethasone release from nonfouling sensor coatings affect the foreign body response. J Biomed Mater Res A 2007;81(4):858-69.

111.   Ju YM, Yu B, Koob TJ, Moussy Y, Moussy F. A novel porous collagen scaffold around an implantable biosensor for improving biocompatibility. I. In vitro/in vivo stability of the scaffold and in vitro sensitivity of the glucose sensor with scaffold. J Biomed Mater Res 2007;in press.

112.   Dungel P, Long N, Yu B, Moussy Y, Moussy F. Study of the effects of tissue reactions on the function of implanted glucose sensors. J Biomed Mater Res A 2007.

113.   Wilson GS, Zhang Y, Reach G, Moatti-Sirat D, Poitout V, Thevenot DR, Lemonnier F, Klein JC. Progress toward the development of an implantable sensor for glucose. Clin Chem 1992;38(9):1613-7.

114.   Updike SJ, Shults MC, Gilligan BJ, Rhodes RK. A subcutaneous glucose sensor with improved longevity, dynamic range, and stability of calibration. Diabetes Care 2000;23(2):208-14.

115.   Moatti-Sirat D, Capron F, Poitout V, Reach G, Bindra DS, Zhang Y, Wilson GS, Thevenot DR. Towards continuous glucose monitoring: in vivo evaluation of a miniaturized glucose sensor implanted for several days in rat subcutaneous tissue. Diabetologia 1992;35(3):224-30.

116. Kissinger   PT.   Biosensors-a   perspective.   Biosens   Bioelectron 2005;20(12):2512-6.

117.   Yoon JJ, Kim JH, Park TG. Dexamethasone-releasing biodegradable polymer scaffolds fabricated by a gas-foaming/salt-leaching method. Biomaterials 2003;24(13):2323-9.

118.   Schleimer R, Busse W, O'Brien P. Inhaled glucocorticoids in asthma. In: Swarbrick J, Boylon JC, editors. Encyclopedia of pharmaceutical technology 1997;New York, Basel: Maecel Dekker:1-29.

119.   Kim D-H, Martin DC. Sustained release of dexamethasone from hydrophilic matrices using PLGA nanoparticles for neural drug delivery. Biomaterials 2006;27:3031-3037.

120.   Gomez-Gaete C, Tsapis N, Besnard M, Bochot A, Fattal E. Encapsulation of dexamethasone into biodegradable polymeric nanoparticles. Int J Pharm 2007;331(2):153-9.

121.   Sanders LM, Kell BA, McRae GI, Whitehead GW. Prolonged controlled-release of nafarelin, a luteinizing hormone-releasing hormone analogue, from biodegradable polymeric implants: influence of composition and molecular weight of polymer. J Pharm Sci 1986;75(4):356-60.

122.   Heya T, Okada H, Ogawa Y, Toguchi H. In vitro and in vivo evaluation of thyrotrophin releasing hormone release from copoly(dl-lactic/glycolic acid) microspheres. J Pharm Sci 1994;83(5):636-40.

123.   Bourke SL, Al-Khalili M, Briggs T, Michniak BB, Kohn J, Poole-Warren LA. A photo-crosslinked poly(vinyl alcohol) hydrogel growth factor release vehicle for wound healing applications. AAPS PharmSci 2003;5(4):E33.

124.   Wu YC, Shaw SY, Lin HR, Lee TM, Yang CY. Bone tissue engineering evaluation based on rat calvaria stromal cells cultured on modified PLGA scaffolds. Biomaterials 2006;27(6):896-904.

125.   Mikos AG, Sarakinos G, Leite SM, Vacanti JP, Langer R. Laminated three-dimensional biodegradable foams for use in tissue engineering. Biomaterials 1993;14(5):323-30.

126.   Richardson TP, Murphy WL, Mooney DJ. Polymeric delivery of proteins and plasmid DNA for tissue engineering and gene therapy. Crit Rev Eukaryot Gene Expr 2001;11(1-3):47-58.

127.   Leach RE, Henry RL. Reduction of postoperative adhesions in the rat uterine horn model with poloxamer 407. Am J Obstet Gynecol 1990;162(5):1317-9.

128.   Steinleitner A, Lambert H, Kazensky C, Cantor B. Poloxamer 407 as an intraperitoneal barrier material for the prevention of postsurgical adhesion formation and reformation in rodent models for reproductive surgery. Obstet Gynecol 1991;77(1):48-52.

129.   Steinleitner A, Lopez G, Suarez M, Lambert H. An evaluation of Flowgel as an intraperitoneal barrier for prevention of postsurgical adhesion reformation. Fertil Steril 1992;57(2):305-8.

130.   Yamaoka T, Takahashi Y, Fujisato T, Lee CW, Tsuji T, Ohta T, Murakami A, Kimura Y. Novel adhesion prevention membrane based on a bioresorbable copoly(ester-ether) comprised of poly-L-lactide and Pluronic: in vitro and in vivo evaluations. J Biomed Mater Res 2001;54(4):470-9.

131.   Wanka G, Hoffmann H, Ulbricht W. Phase Diagrams and Aggregation Behavior of Poly(oxyethylene)-Poly(oxypropylene)-Poly(oxyethylene) Triblock Copolymers in Aqueous Solutions. Macromolecules 1994;27(15):4145 - 4159.

132.   Oh SH, Kim JK, Song KS, Noh SM, Ghil SH, Yuk SH, Lee JH. Prevention of postsurgical tissue adhesion by anti-inflammatory drug-loaded pluronic mixtures with sol-gel transition behavior. J Biomed Mater Res A 2005;72(3):306-16.

133.   Fu Y-J, Shyu S-S, Su F-H, Yu P-C. Development of biodegradable co-poly(-lactic/glycolic acid) microspheres for the controlled release of 5-FU by the spray drying method. Colloids Surf., B Biotinerfaces 2002;25:269-279.

121

APPENDICES

Appendix A: Protocol – Preparation Procedure of Coil-type Glucose Sensors

A.1. Coiling of Platinum-iridium (Pt-Ir) Wires

- Cut 0.125 mm Pt-Ir wires into 4-7 cm long.

- Remove the top Teflon tube (1 cm).

- Polish the bare wire with a swab in toothpaste.

- Ultrasonic cleaning the platinum surface in pure water for 5 min.

- Coil the stripped wire around a 30 G1/2 needle.

- Ultrasonic cleaning the platinum surface in pure water for 5 min. again.

- Carefully pass through a cotton thread the coils then cut the two ends of the thread, do not let any cotton silks leave out the coils.

A.2. Enzyme Coating

- Glucose oxidase solution preparation:

    300 µL pure water

    12 mg Bovine serum albumin (BSA)

    2.5 mg glucose oxidase (GOD)

    4 µL glutaraldehyde (50% v/v)

- Dip-coatings (3 times).

- Let it dry 1 hour at room temperature.

Appendix A (Continued)

A.3. Epoxy-PU Coating

- Coating solution preparation:

      Tetrahydrofunan (THF) 4 mL

      PU 45 mg

      Brij30 5mg

      Epoxy adhesives 50mg

- Dip-coatings (3 times) & Dry at room temperature for 30-60 min.

- Coat two-end of coil & Dry at room temperature for 30-60 min.

- Cure at 80-120°C for 60 min.

- Place in PBS prior to use (at least 1 day for membrane swelling).

Appendix B: Protocol – Measurement of Sensor Function

B.1. Preparation of Measurement

- Testing solution:

    PBS

    5 mM glucose/PBS solution

    100 mM glucose/PBS solution

- Potentiostat options:

    Select chronoamperometry

    Set applied potential at 0.7V

- Cell setup:

    8 ml of 5 mM glucose/PBS in a 10 mL glass beaker

    Connect counter and reference clamps to the Ag/AgCl electrode

    Connect working electrode to the glucose sensor

B.2. Response Time and Slope Measurement

- Run the program until the current (I_{5mM}) reach a stable level.

- Add 941 µL of 100 mM Glucose/PBS into the cell and continue to record the current change until the second current (I_{15mM}) level stable.

- Response time may be expressed as $T_{95\%}$(sec.) [Fig. B.1].

- Sensitivity (S) can be roughly calculated by:

    S (nA/mM) = (I_{15mM} - I_{5mM}) / (C_{15mM} - C_{5mM}) = ΔI / 10

125
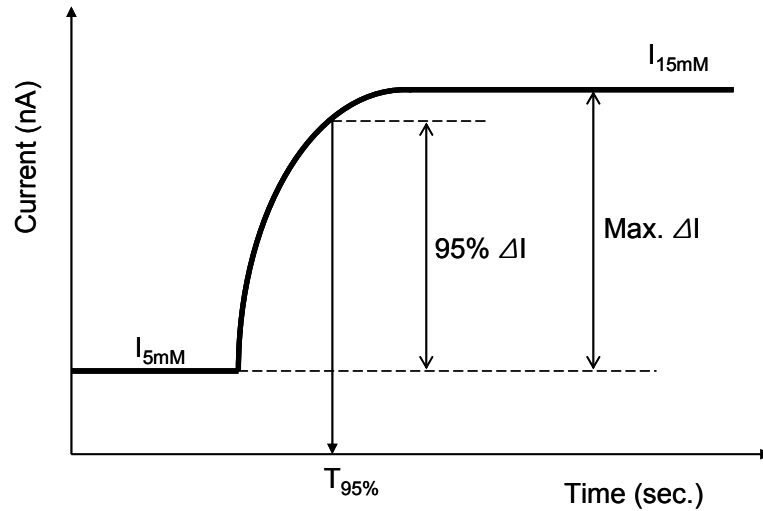
Figure B.1. Amperometric Response Curve.

B.3. Preparation of Calibration Plot

- Run the program until the background current reach a stable level.

- Step-add x µL of 100mL Glucose/PBS into the cell every 500 sec.

- Obtained a group of corresponding currents ($I1 - I7$).

- Draw the current-concentration dependence.

- Response sensitivity can be obtained by calculating the slope of the current (I)

  vs glucose concentration (C) linearity relationship.

126

Appendix B (Continued)

Table B.1. Changes of Glucose Concentration in the Cell.

X (mL) of 100 mM glucose/PBS solution	Glucose concentration (mM)	Current (nA)
0.163	2	I1
0.258	5	I2
0.467	10	I3
0.523	15	I4
0.589	20	I5
0.667	25	I6
0.762	30	I7

Appendix C: Protocol – Implantation of Glucose Sensors in the Rat and Measurement of Sensor Function *In vivo*

C.1. Surgery Materials

- Male Sprague Dawley Out bred Rats (375g – 399 grams).

- Isofluorane anesthesia machine.

- Surgical clippers and water circulating heating board.

- Sterile bench pads, drapes, surgery packs with scalpels, and probes.

- 3-0 Proline sutures.

- Sterile and non-sterile gloves.

- Lab note book, pen and sharpie.

- Sterile and un-sterile gauze.

- Puralube ointment for eyes.

- 50cc of D50 glucose solution.

- Sterile towels (to keep animal warm).

- Chlorhexidine / Betadine solutions.

- Isopropyl alcohol.

- 50cc of D50 glucose solution.

C.2. Glucose Monitoring and Testing Apparatus

- Apollo 4000 Free Radical Analyzer.

- FreeStyle Blood Glucose Monitoring System.

Appendix C (Continued)

C.3. Sterilization and Pre-calibration of Glucose Sensors

- All sensors will be sterilized by 70% ethanol.

- Each sensor will be incubated in a sterile 5mM glucose solution three days before implantation.

- On the day before implantation, each sensor will be pre-calibrated with 5 mM and 15mM glucose solutions which are sterilized by a sterile syringe filter.

- After obtaining the sensitivity value of each individual sensor, the sensor will be stored in sterile distilled water.

C.4. Protocol for Animal Surgery

- All surgical instruments and other items to be sterilized will be autoclaved at 260°C for 25 min. doubled wrapped or in the sterilization pouch.

- Surgery will be conducted on a clean surface wiped with disinfectant before and after use.

- A Continuous Flow Gas Anesthesia System (flow meter, vaporizer, tubing and connectors) will be used to deliver Isoflourane to the rats. The animals will first be placed in an induction chamber for induction of anesthesia and then the gas will be delivered through a rat mask when surgery is performed. Position the first rat on the water circulating heating board for rodents using tape to insure positioning of the body, head and rat mask.

129

Appendix C (Continued)

- Each of the rats that are under anesthesia will have their eyes lubricated with Puralube ointment.

C.5. Implantation of Sensors (Long Wire Sensors)

- An area on the dorsal aspect of each rat will be shaved at the cervical region to the lumbar region.

- The skin will be surgically prepped using 3 scrubs of 2% Chlorhexidine and painted with Betadine and left to dry.

- A sterile fenestrated drape will be placed on the rat.

- Each rat will have 2 sensors implanted.

- Using the scissors a 1.5 cm incision is made at the dorsal midline 3cm below the inter-scapular area. Lateral incisions are made 1cm below the inter-scapular area 1cm lateral to the dorsal midline on either side.

- The 14-gauge. I.V. catheter was inserted subcutaneously toward the incision from the 4 - 5 cm lower back region.

- Withdraw the 14-gauge needle leaving the catheter in place.

- The sensor can then be carefully advanced, using thumb and forceps, through the catheter without touching the distal end of the sensor.

- The sensor was secured to the skin by passing a 3-0 Prolene suture through the small gap of the wound clip on the sensor wires.

- The incision was sutured using 3-0 Prolene.

130

Appendix C (Continued)

- The cannula was then retracted, leaving the sensor in the subcutaneous tissue.

- The sensor was secured to the skin by passing a 3-0 Prolene suture through the small gap of the wound clip on the sensor wires.

- The incision was sutured using 3-0 Prolene.

- The cannula was then retracted, leaving the sensor in the subcutaneous tissue (For short wire sensors - the sensors were directly implanted through the incision without using a cannula).

C.6. Sensors Testing

- Sensor testing will be performed with two anesthetized rats at a time. A total of 8 sensors will be tested per day.

- The implanted sensors wires will be attached to the Apollo 4000 potentiostat and a 0.7V *vs*. Ag/AgCl potential will be applied to four sensors. At the same time, four response current curves will be continuously recorded on digital display.

- After the one hour "run-in period" is complete a relatively stable signal (I_1) from the sensors will be recorded.

- Using the Freestyle™ glucometer, the low blood glucose level (C_1) will established using 1/3 micro liter of blood from the rat tail.

131

- After a stable signal is obtained from the sensors, 2.0 g/kg rat body weight of 50% glucose/water solution will be administered intraperitoneally using a 27 gauge IV needle.

- An increase in the blood glucose of the rat will correspond with a rise in the slope of the current-time curve of each sensor. Previous *in vivo* studies have demonstrated that plasma glucose will increase to a plateau (I_2). This time interval is long enough to establish equilibrium between plasma and subcutaneous glucose concentrations.

- More blood tests will be made every 5-10 minutes after injection of glucose until the high glucose level (C_2) is stable.

- A blood-calibrated sensitivity (S) can be calculated:

  S (nA / mM) = I_2 - I_1 / C_2 - C_1

- The same test will be performed on days 7, 14, 21, and 28 to establish the sensitivity of the sensors over time.

C.7. Animal Recovery

- Remove the animal from the anesthesia device.

- Gently place the animal back into its cage.

- Place half the cage onto a circulating heating broad or place an electric heating pad in the cage to cover half the area of the cage floor.

Appendix C (Continued)

- Once fully recovered from anesthesia, replace the water, food, but no toys or
  tunnels in the cage with the animal.

- Daily observation of the rats with notes in the lab book should be done.

ABOUT THE AUTHOR

Young Min Ju received a Bachelor of Science in Macromolecular Science from Hannam University (South Korea) in 1996. He continued to study in the Biomedical Polymers at the graduate school of his alma mater. While in graduate school years, he was assigned as a research and teaching assistant under the supervision of Dr. Jin Ho Lee. After earning a Master of Science in Macromolecules in 1999, He worked as a research scientist at the Biomaterials Research Center in the Korea Institute of Science & Technology (KIST) until summer 2003. He entered the Ph.D. in Biomedical Engineering Program at the University of South Florida in fall 2003 and worked as research assistant in the Biosensor and Biomaterials Lab. under the supervision of Dr. Francis Moussy.